



# Dietary Docosahexaenoic Acid Prevents Silica-Induced Development of Pulmonary Ectopic Germinal Centers and Glomerulonephritis in the Lupus-Prone NZBWF1 Mouse

## OPEN ACCESS

### Edited by:

J. Michelle Kahlenberg,  
University of Michigan, United States

### Reviewed by:

Jason Weinstein,  
Yale University, United States  
Theresa T. Lu,  
Hospital for Special Surgery,  
United States

### \*Correspondence:

Jack R. Harkema  
harkemaj@msu.edu  
James J. Pestka  
pestka@msu.edu

†These authors have contributed  
equally to this work

### Specialty section:

This article was submitted to  
Autoimmune and Autoinflammatory  
Disorders,  
a section of the journal  
Frontiers in Immunology

Received: 10 May 2018

Accepted: 14 August 2018

Published: 12 September 2018

### Citation:

Bates MA, Akbari P, Gilley KN,  
Wagner JG, Li N, Kopec AK,  
Wierenga KA, Jackson-Humbles D,  
Brandenberger C, Holian A,  
Benninghoff AD, Harkema JR and  
Pestka JJ (2018) Dietary  
Docosahexaenoic Acid Prevents  
Pulmonary Ectopic Germinal Centers  
and Glomerulonephritis in the  
Lupus-Prone NZBWF1 Mouse.  
Front. Immunol. 9:2002.  
doi: 10.3389/fimmu.2018.02002

Melissa A. Bates<sup>1,2†</sup>, Peyman Akbari<sup>1,2,3†</sup>, Kristen N. Gilley<sup>1</sup>, James G. Wagner<sup>3</sup>, Ning Li<sup>3</sup>, Anna K. Kopec<sup>2,3</sup>, Kathryn A. Wierenga<sup>2,4</sup>, Daven Jackson-Humbles<sup>3</sup>, Christina Brandenberger<sup>5</sup>, Andrij Holian<sup>6</sup>, Abby D. Benninghoff<sup>7</sup>, Jack R. Harkema<sup>2,3\*</sup> and James J. Pestka<sup>1,2,8\*</sup>

<sup>1</sup> Department of Food Science and Human Nutrition, Michigan State University, East Lansing, MI, United States, <sup>2</sup> Institute for Integrative Toxicology, Michigan State University, East Lansing, MI, United States, <sup>3</sup> Department of Pathobiology and Diagnostic Investigation, Michigan State University, East Lansing, MI, United States, <sup>4</sup> Department of Biochemistry and Molecular Biology, Michigan State University, East Lansing, MI, United States, <sup>5</sup> Institute of Functional and Applied Anatomy, Hannover Medical School, Hannover, Germany, <sup>6</sup> Department of Biomedical and Pharmaceutical Sciences, Center for Environmental Health Sciences, University of Montana, Missoula, MT, United States, <sup>7</sup> Department of Animal, Dairy and Veterinary Sciences, School of Veterinary Medicine, Utah State University, Logan, UT, United States, <sup>8</sup> Department of Microbiology and Molecular Genetics, Michigan State University, East Lansing, MI, United States

Ectopic lymphoid structures (ELS) consist of B-cell and T-cell aggregates that are initiated *de novo* in inflamed tissues outside of secondary lymphoid organs. When organized within follicular dendritic cell (FDC) networks, ELS contain functional germinal centers that can yield autoantibody-secreting plasma cells and promote autoimmune disease. Intranasal instillation of lupus-prone mice with crystalline silica (cSiO<sub>2</sub>), a respirable particle linked to human lupus, triggers ELS formation in the lung, systemic autoantibodies, and early onset of glomerulonephritis. Here we tested the hypothesis that consumption of docosahexaenoic acid (DHA), an ω-3 polyunsaturated fatty acid with anti-inflammatory properties, influences the temporal profile of cSiO<sub>2</sub>-induced pulmonary ectopic germinal center formation and development of glomerulonephritis. Female NZBWF1 mice (6-wk old) were fed purified isocaloric diets supplemented with 0, 4, or 10 g/kg DHA - calorically equivalent to 0, 2, or 5 g DHA per day consumption by humans, respectively. Beginning at age 8 wk, mice were intranasally instilled with 1 mg cSiO<sub>2</sub>, or saline vehicle alone, once per wk, for 4 wk. Cohorts were sacrificed 1, 5, 9, or 13 wk post-instillation (PI) of the last cSiO<sub>2</sub> dose, and lung and kidney lesions were investigated by histopathology. Tissue fatty acid analyses confirmed uniform dose-dependent DHA incorporation across all cohorts. As early as 1 wk PI, inflammation comprising of B (CD45R<sup>+</sup>) and T (CD3<sup>+</sup>) cell accumulation was observed in lungs of cSiO<sub>2</sub>-treated mice compared to vehicle controls; these responses intensified over time. Marked follicular dendritic cell (FDC; CD21<sup>+</sup>/CD35<sup>+</sup>) networking appeared at 9 and 13 wk PI. IgG<sup>+</sup> plasma cells suggestive of mature germinal centers were evident at 13 wk.

DHA supplementation dramatically suppressed cSiO<sub>2</sub>-triggered B-cell, T-cell, FDC, and IgG<sup>+</sup> plasma cell appearance in the lungs as well as anti-dsDNA IgG in bronchial lavage fluid and plasma over the course of the experiment. cSiO<sub>2</sub> induced glomerulonephritis with concomitant B-cell accumulation in the renal cortex at 13 wk PI but this response was abrogated by DHA feeding. Taken together, realistic dietary DHA supplementation prevented initiation and/or progression of ectopic lymphoid neogenesis, germinal center development, systemic autoantibody elevation, and resultant glomerulonephritis in this unique preclinical model of environment-triggered lupus.

**Keywords:** autoimmunity, ectopic lymphoid structure, omega-3, polyunsaturated fatty acid, systemic lupus erythematosus, silica, lung

## INTRODUCTION

Systemic lupus erythematosus (lupus) is a heterogeneous autoimmune disease (AD) that primarily affects young women causing great individual suffering and social costs (1, 2). Induction and progression of this disease is coordinated by aberrant activation of innate and adaptive immunity. Pathogenesis involves loss of tolerance to self-antigens, activation of autoreactive B- and T-cells and consequent production of pathogenic autoantibodies (3). The latter complex with self-antigens such as dsDNA, forming circulating immune complexes that amass within tissues. In the kidney, these complexes drive mononuclear cell infiltration and activation, promoting glomerulonephritis that often culminates in end-stage renal disease (4).

During unresolved inflammation, ectopic lymphoid structures (ELS) are induced to remediate high concentrations of locally-present antigens in inflamed tissue and, thus, do not occur in pre-programmed locations in the body. Also known as tertiary lymphoid organs, ELS operate much like secondary lymphoid organs; they serve structurally and functionally as a site for antigen accumulation, presentation, and proliferation/activation of B- and T-cells. B- and T-cell-rich areas are distinct with the former being supported within a matrix of follicular dendritic cells (FDCs) (5–7). Unlike hematopoietic myeloid and plasmacytoid dendritic cells, FDCs are considered mesenchymal in nature. They express low levels of major histocompatibility complex (MHC) II and are identified by their surface expression of FcγRIIb, complement receptor (CR) 1 (CD35), and CR2 (CD21) [reviewed in (8)]. These receptors facilitate FDC presentation of immune complexes of antibody or complement-opsonized antigens. FDCs dictate the fate of B-cells in germinal centers by serving as a platform for their recruiting, activation, differentiation, and survival (9). Importantly, ELS are frequently associated with lupus and other ADs reflecting the intimate

association between aberrant inflammation and loss of self-tolerance. ELS are found in AD target tissues such as kidneys (lupus), salivary glands (Sjögren's syndrome), and synovial joints (rheumatoid arthritis) and correlate with disease severity (6, 10–14).

Although lupus and other ADs are driven by an individual's genome, environmental factors such as toxicants and diet can influence onset and severity of autoimmunity (15–20). Regarding toxicants, it is well-established that inhaled crystalline silica dust (cSiO<sub>2</sub>, quartz) can contribute to AD onset and progression [reviewed in (21)]. Approximately 2.3 million individuals who work in occupations such as mining, construction, manufacturing, and farming are exposed to respirable cSiO<sub>2</sub> (22). Airway exposure to cSiO<sub>2</sub> evokes overt and chronic inflammation that affects not only the lung, but also distal organs by way of systemic inflammation (23, 24). Epidemiological studies have linked cSiO<sub>2</sub> exposure to lupus, rheumatoid arthritis, Sjögren's syndrome, scleroderma, and systemic vasculitis (25–29).

Animal studies provide mechanistic insight into how cSiO<sub>2</sub> might trigger autoimmunity in humans (30–33). Intranasal cSiO<sub>2</sub> instillation of the female NZBWF1 mouse, a widely used murine model of human lupus (34), induces autoimmunity and glomerulonephritis 3 months earlier than vehicle-instilled controls (35). Concurrently, there are massive inflammatory responses in the lungs as evidenced by intense perivascular and peribronchial lymphocytic cell infiltration. These infiltrates contain many B (CD45R<sup>+</sup>) cells and T (CD3<sup>+</sup>) cells indicative of ectopic lymphoid neogenesis. Consistent with pulmonary inflammation and ELS formation, bronchoalveolar lavage fluid (BALF) from cSiO<sub>2</sub>-exposed mice contain elevated concentrations of IgG, autoantibodies, chemokines, and cytokines. These responses are similarly reflected in the plasma and, therefore, indicative of parallel exacerbation of systemic autoimmunity. Overall, these findings strongly indicate that the lung acts as a platform for autoimmune triggering by cSiO<sub>2</sub>.

Dietary intake of polyunsaturated fatty acids (PUFAs) may have considerable influence on inflammation and autoimmunity [reviewed in (36)]. PUFAs that have two or more double bonds are designated as ω-3 or ω-6 based on the position of the first double bond relative to the aliphatic chain's terminal carbon. Generally, ω-3 PUFAs are recognized to be anti-inflammatory in nature, whereas ω-6 PUFAs are regarded as proinflammatory

**Abbreviations:** AD, autoimmune disease; ARA, arachidonic acid; BALF, bronchoalveolar lavage fluid; cSiO<sub>2</sub>, crystalline silica; CON, control; DHA, docosahexaenoic acid; ELS, ectopic lymphoid structure; EPA, eicosapentaenoic acid; FA, fatty acid; FDC, follicular dendritic cell; HRP, horseradish peroxidase; GLC, gas liquid chromatography; LA, linoleic acid; PBS, phosphate buffered saline; PI, post-instillation; PUFA, polyunsaturated fatty acid; RT, room temperature; SPMs, specific pro-resolving metabolite; VEH, vehicle.

(37). Linoleic acid (C18:2  $\omega$ -6; LA), the most common PUFA in the Western diet, is present in food oils produced from plants such as corn and soybeans. After consumption by ruminants and humans, LA can be elongated and desaturated enzymatically to arachidonic acid (C20:4  $\omega$ -6; ARA). Thus, LA and ARA are major components of cell membrane phospholipids. Even though the  $\omega$ -3 PUFA  $\alpha$ -linolenic acid (C18:3  $\omega$ -3; ALA) is additionally present in plant oils, humans and other mammals have limited ability to elongate it enzymatically to more anti-inflammatory forms, docosahexaenoic acid (C22:6  $\omega$ -3; DHA) and eicosapentaenoic acid (C20:5  $\omega$ -3; EPA). Therefore, humans need to obtain these PUFAs from exogenous sources. Several marine algae proficiently catalyze formation of DHA and EPA, and cold-water fish consuming these algae efficiently bioconcentrate these PUFAs into their tissues (38). Accordingly, fish, fish oil, and microalgal oil are significant sources of DHA and EPA in the human diet (39).

Numerous preclinical investigations have demonstrated that  $\omega$ -3 PUFA-rich fish oil supplementation both prevents and resolves inflammation [reviewed in (40, 41)]. Therefore, its consumption might also benefit people with a genetic predisposition to AD. In support of this contention, fish oil supplementation of lupus-prone mice prevents or delays glomerulonephritis and death from kidney failure, with DHA-enriched fish oil having the greatest potency (42–50). In a prior work, we compared latency and severity of autoimmunity in female NZBWF1 mice consuming (1) an  $\omega$ -3 PUFA-rich diet containing DHA-enriched fish oil, (2) an  $\omega$ -6 PUFA-rich Western-type diet containing corn oil, or (3) an  $\omega$ -9 monounsaturated fatty acid (MUFA)-rich Mediterranean-type diet containing high oleic safflower oil (51). While increases of plasma autoantibodies, proteinuria, and glomerulonephritis were readily evident in mice consuming  $\omega$ -6 PUFA or  $\omega$ -9 MUFA diets, these outcomes were remarkably lessened in animals fed the DHA-rich diet. These inhibitory effects correlated with downregulation of genes associated with inflammatory responses, antigen presentation, T-cell activation, B-cell activation/differentiation and leukocyte recruitment. Importantly, a large number of these genes are specific targets for lupus intervention.

Recently, we queried how DHA supplementation influences cSiO<sub>2</sub>-induced autoimmunity in female NZBWF1 mice. Dietary DHA at concentrations that were calorically equivalent to 2, 6, and 12 g per day human consumption dose-dependently suppressed cSiO<sub>2</sub>-triggered inflammation, accumulation of pulmonary B- and T-cell aggregates, autoimmunity, and glomerulonephritis (52). While these observations offer the intriguing possibility that DHA supplementation could be used to block environment-triggered lupus, such an interpretation is constrained because the investigation focused only on a single time point—3 months following the final cSiO<sub>2</sub> instillation and after glomerulonephritis onset. Furthermore, the presence of B- and T-cell aggregates was not explicitly linked to the presence of FDCs and plasma cells. To address these knowledge gaps, in the present study we determined how dietary DHA supplementation, at two concentrations

that realistically mimic safe human consumption (2 and 5 g per day), influences the temporal profile of cSiO<sub>2</sub>-triggered (1) pulmonary B-cells, T-cells, FDCs, and plasma cells indicative of ectopic germinal centers, (2) systemic autoimmunity, and (3) glomerulonephritis in the female NZBWF1 lupus model.

## MATERIALS AND METHODS

### Animals and Diets

All experimental protocols were reviewed and approved by the Institutional Animal Care and Use Committee at Michigan State University in accordance with the National Institutes of Health guidelines (AUF #01/15-021-00). Female 6-wk-old lupus-prone NZBWF1 mice were obtained from The Jackson Laboratories (Bar Harbor, ME), housed four per cage with free access to food and water, and kept at constant temperature (21–24°C) and humidity (40–55%) under a 12 h light/dark cycle.

Upon arrival and for the duration of the study, mice were fed one of four experimental diets (Table 1). Formulations were based on the semi-purified American Institute of Nutrition (AIN)-93G containing 70 g/kg fat (53). To provide basal essential fatty acids (FAs), all diets contained 10 g/kg corn oil. Control diet (CON) was formulated with 60 g/kg high-oleic safflower oil (Hain Pure Food, Boulder, CO). To prepare DHA-enriched diets, high-oleic safflower oil was substituted with 10 g/kg (Low DHA) or 25 g/kg (High DHA) microalgal oil containing 40% DHA (DHASCO, kindly provided by Dr. Kevin Hadley, DSM Nutritional Products, Columbia MD). This yielded experimental diets that contained 4 or 10 g/kg DHA, respectively, and modeled,

TABLE 1 | Diet formulations.

	CON	Low DHA <sup>e</sup>	High DHA <sup>f</sup>
Casein	200	200	200
Dyetrose	132	132	132
Cornstarch	397.5	397.5	397.5
Sucrose	100	100	100
Cellulose	50	50	50
t-Butylhydroquinone (TBHQ)	0.01	0.01	0.01
AIN 93G Salt Mix	35	35	35
AIN 93G Vitamin Mix (with Vitamin E)	10	10	10
L-cysteine	3	3	3
Choline Bitartrate	2.5	2.5	2.5
Corn Oil <sup>a,b</sup>	10	10	10
High-oleic safflower Oil <sup>a,c</sup>	60	50	35
DHA-Enriched Algal Oil <sup>a,d</sup>	–	10	25

Values shown are the mass amounts (g) per kg diet.

<sup>a</sup> Based on oil composition reported by the manufacturer.

<sup>b</sup> Corn oil contained 612 g/kg linoleic acid and 26 g/kg oleic acid.

<sup>c</sup> High-oleic safflower oil contained 750 g/kg oleic acid and 140 g/kg linoleic acid.

<sup>d</sup> Algal oil contained 395 g DHA/kg and 215 g oleic acid/kg.

<sup>e</sup> 4 g/kg diet, calorically equivalent to human DHA consumption of 2 g/day.

<sup>f</sup> 10 g/kg diet, calorically equivalent to human DHA consumption of 5 g/day.

on a caloric basis, human DHA consumption of 2 and 5 g per day, respectively.

## Experimental Design

The experimental design for this study is depicted in **Figure 1**. At 6 wk of age, groups of mice ( $n = 8$ ) were fed CON, Low DHA, or High DHA diets and maintained on assigned diets until the end of the experiment. To prevent the formation of lipid oxidation products, diets were mixed weekly and stored at  $-20^{\circ}\text{C}$  until use. Fresh feed was provided ad lib to mice daily. At 8 wk of age, mice were anesthetized with 4% isoflurane and intranasally instilled with 1 mg  $\text{cSiO}_2$  in 25  $\mu\text{l}$  phosphate buffered saline (PBS) or the PBS vehicle (VEH). Exposures were repeated once per wk for 4 wk.  $\text{cSiO}_2$  (Min-U-Sil-5, 1.5–2.0  $\mu\text{m}$  average particle size, Pennsylvania Sand Glass Corporation, Pittsburgh, PA) was acid washed and dried prior to preparation of stock suspensions of  $\text{cSiO}_2$  in VEH. Stock suspensions were prepared fresh in VEH prior to exposure, sonicated, and vortexed rapidly for 1 min prior to intranasal instillation. This dosing regimen reflects approximately one half of a human lifetime exposure at the recommended Occupational Safety and Health Administration limit (35).

Cohorts of mice representing the four treatment groups (i.e., CON/VEH, CON/ $\text{cSiO}_2$ , Low DHA/ $\text{cSiO}_2$ , and High DHA/ $\text{cSiO}_2$ ) were sacrificed at 1, 5, 9, and 13 wk after the final  $\text{cSiO}_2$  instillation. Mice were 12, 16, 20, and 24 wk of age, respectively, at these time points. These time periods were selected to capture pulmonary pathological changes in lupus-prone NZBWF1 mice following  $\text{cSiO}_2$  exposure prior to and during onset of glomerulonephritis based on prior studies (35, 52). Animals were euthanized by intraperitoneal injection with 56 mg/kg body weight sodium pentobarbital and exsanguination via the abdominal aorta. Blood was collected with heparin-coated syringes and centrifuged at  $3500 \times g$  for 10 min at  $4^{\circ}\text{C}$  for separation of erythrocytes and plasma which were

stored at  $-80^{\circ}\text{C}$ . BALF was collected from whole lungs as described previously (54). After lavage, the right lung lobes were removed, frozen in liquid nitrogen, and stored at  $-80^{\circ}\text{C}$  for FDC immunohistochemistry. The left lung lobe was fixed with 10% neutral buffered formalin (Fisher Scientific, Pittsburgh, PA) at constant pressure (30 cm  $\text{H}_2\text{O}$ ) for minimum of 1 h and stored in fixative until further processing for histology. The right kidney was excised and the cranial portion fixed in 10% neutral buffered formalin for 24 h.

## Fatty Acid Analyses

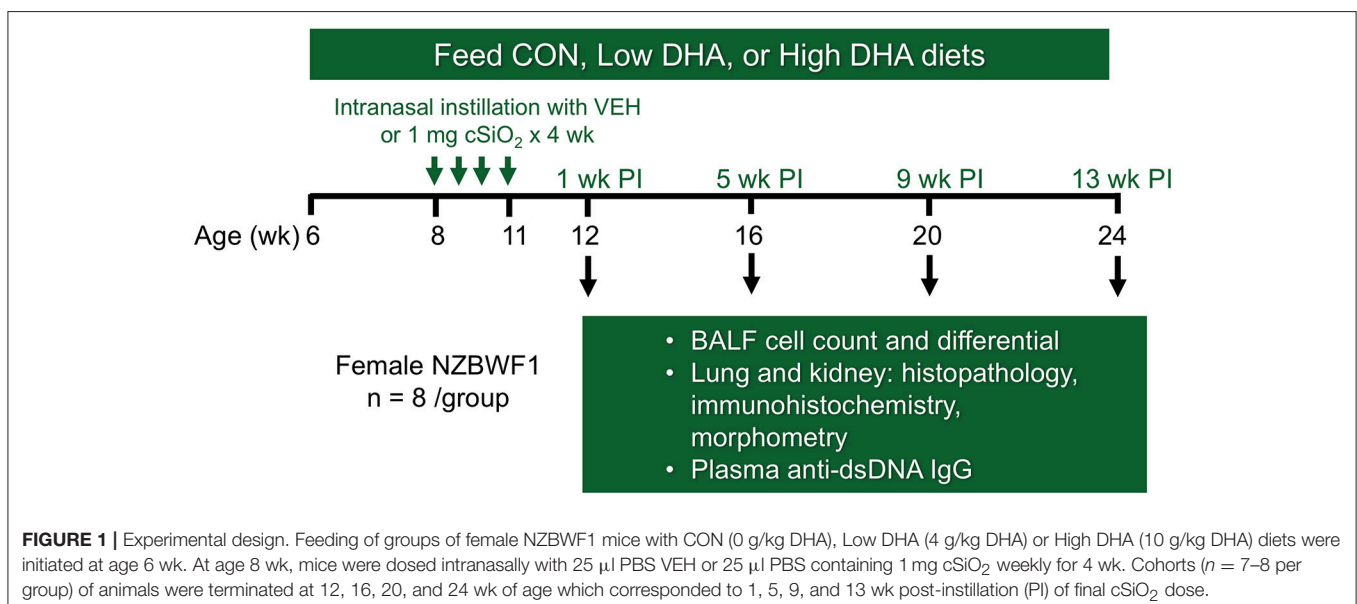
Fatty acid (FA) concentrations in diets were determined by gas liquid chromatography (GLC) as previously described (52). FA data are reported as percentages (w/w) of FAs detected with a chain length between 10 and 24 carbon atoms. The lower limit of detection was  $<0.001$  g/100 g fatty acids. FA concentrations in erythrocytes were analyzed by GLC at Omega Quant (Sioux Falls, SD).

## BALF Cell Counts

Total cells in BALF were determined by counting on a hemocytometer. Cytological slides were prepared by centrifugation of 150  $\mu\text{l}$  BALF for 10 min at  $400 \times g$ , air-drying, and staining with Diff-Quick (Thermo-Fisher). Two hundred (200) cells were counted and designated as monocytes/macrophages, lymphocytes, and eosinophils using morphological criteria.

## Anti-dsDNA IgG Analysis

Anti-dsDNA IgG responses in BALF and plasma were measured using mouse anti-dsDNA IgG-specific ELISA Kit (Alpha Diagnostic International, San Antonio, TX) according to manufacturer's instructions. Briefly, samples as well as standards were added to plate wells, incubated and bound antibody was



measured using horseradish peroxidase (HRP)-labeled anti-mouse IgG. Anti-dsDNA in samples was determined from standard curve generated with mouse anti-dsDNA.

## Histopathology of Lungs and Kidneys

Randomly oriented, serial sections of formalin-fixed left lung lobes were processed routinely and embedded in paraffin. Tissue sections (5  $\mu\text{m}$ ) were deparaffinized and stained with hematoxylin and eosin (H&E) for histopathology. Tissues were scored semi-quantitatively in a blinded fashion by a board-certified veterinary pathologist for the following lung lesions: (a) presence of lymphoid aggregates within perivascular and peribronchiolar regions; (b) histologically evident ectopic lymphoid tissues; (c) presence of alveolar proteinosis; (d) alveolitis defined as the increased accumulation in the alveolar parenchyma of neutrophils, lymphocytes, and mononuclear/macrophages; (e) alveolar type II epithelial cell hyperplasia; and (f) mucous cell metaplasia in bronchiolar epithelium. Individual lungs were graded for these lesions using the following criteria (% of total pulmonary tissue examined): (0) no changes compared to control mice; (1) minimal (<10%); (2) slight (10–25%); (3) moderate (26–50%); (4) severe (51–75%); or (5) very severe (>75%) of total area affected.

Formalin-fixed kidneys were randomly sectioned, paraffin-embedded, cut and stained with either H&E or Periodic acid-Schiff and hematoxylin (PASH). Stained sections were evaluated for lupus nephritis by a board-certified veterinary pathologist using a modified International Society of Nephrology/Renal Pathology (ISN/RPS) Lupus Nephritis Classification system (55). Slide sections were graded as follows: (0) no tubular proteinosis and normal glomeruli; (1) mild tubular proteinosis with multifocal segmental proliferative glomerulonephritis and occasional early glomerular sclerosis and crescent formation; (2) moderate tubular proteinosis with diffuse segmental proliferative glomerulonephritis, early glomerular sclerosis and crescent formation; and (3) marked tubular proteinosis with diffuse global proliferative and sclerosing glomerulonephritis. The extent of tubular necrosis was measured in PASH-stained slides by morphometry as described below.

## Immunohistochemistry of Lungs and Kidneys

Immunohistochemistry was performed on formalin-fixed, paraffin embedded, left lung lobe and right kidney for identification of CD45R<sup>+</sup> (B-cells). Sections were cut at 7  $\mu\text{m}$  on a microtome and placed on slides coated with 2% 3-aminopropyltriethoxysilane and dried at 56°C overnight. Slides were deparaffinized in xylene and rehydrated through descending grades of ethyl alcohol to distilled water followed by Tris Buffered Saline (TBS) (pH 7.4) without surfactant (Scytek Labs, Logan, UT) for 5 min for pH adjustment. Following TBS treatment, paraffin-embedded tissue sections underwent heat induced epitope recovery with Citrate Plus Retrieval pH 6.0 (Scytek Labs) for 30 mins at 125°C followed by a 30 min incubation at room temperature (RT). Endogenous peroxidase was blocked with 3% hydrogen peroxide and methanol (1:4) for 30 min followed by tap and distilled water rinses.

After pretreatments, standard micro-polymer complex staining was performed at RT on an IntelliPath Flex Autostainer (Biocare Medical, Pacheco, CA). All staining steps were followed by rinses in TBS autowash buffer (Biocare). After blocking for non-specific protein with Rodent Block M (Biocare) for 20 min, sections were incubated with 1:600 rat anti-CD45R monoclonal antibody (Becton Dickinson, Franklin Lakes, NJ; catalog # 550286) in normal antibody diluent (Scytek) for 1 h to identify B-cells. Bound CD45R antibody was detected with ProMark Rat-on-Mouse HRP Polymer by 30 min incubations with probe and polymer, respectively, and reaction developed with Romulin 3-amino-9-ethylcarbazole (AEC) chromogen (Scytek) prior to being counterstained with 1:10 hematoxylin for 1 min followed by distilled water. Slides were air dried and cover slips then applied with permanent synthetic mounting media.

For identification of CD3<sup>+</sup> (T-cells) in lung parenchyma, following deparaffinization and rehydration, tissue sections underwent heat induced epitope retrieval with Citrate Plus Retrieval pH 6.0 (Scytek) for 30 min at 100°C followed by a 10 min incubation at RT. Endogenous peroxidase was blocked as described above, and non-specific binding was blocked with Rodent Block M for 10 min. After pretreatments, 1:250 rabbit anti-CD3 polyclonal antibody (Abcam, Cambridge, MA; catalog #ab5690) was incubated for 1 h to identify T-cells. Bound CD3 antibody was detected with ProMark Rat-on-Mouse HRP polymer (Biocare) with 15 min incubation for probe and polymer, respectively and reaction developed with AEC for 5 min prior to being counterstained with hematoxylin.

For detection of IgG<sup>+</sup> cells in lung, deparaffinized sections were incubated with 0.03% pronase E for 10 min at 37°C to achieve antigen retrieval and then endogenous peroxidase inactivated as described above. After blocking for non-specific protein with Rodent Block M (Biocare) sections were incubated with 1:100 polyclonal goat anti-IgG (Bethyl Labs, Montgomery, TX; catalog# A-90-100A) for 30 min. Goat-specific Micro-Polymer (Biocare) reagents were subsequently applied as per manufacturer's instructions, followed by reaction development with Romulin AEC<sup>TM</sup> (Biocare) and counterstained with hematoxylin.

Immunohistochemistry for CD21<sup>+</sup>/CD35<sup>+</sup> (FDC) was performed on snap frozen cranial lobe of the right lung. Tissues were sectioned at 7  $\mu\text{m}$  and sections air dried overnight on 2% 3-aminopropyltriethoxysilane coated slides. Sections were fixed with acetate and formalin for 10 min at RT, and endogenous peroxidase was blocked using 3% hydrogen peroxide in TBS for 30 min. Blocking for non-specific binding was performed with Rodent Block M (Biocare) for 5 min. Following pretreatments, 1:500 rat anti-CD21/35 monoclonal antibody (Becton Dickinson; catalog # 553817) was incubated for 1 h to identify FDCs. Bound CD21/CD35 antibody was detected with ProMark Rat-on-Mouse HRP polymer (Biocare) with 15 min incubation for probe and polymer, respectively and reaction developed with AEC for 5 min prior to being counterstained with hematoxylin.

## Morphometry

To quantitate immunohistochemically labeled cells in lungs (CD45R<sup>+</sup>, CD3<sup>+</sup>, and CD21<sup>+</sup>/CD35<sup>+</sup>) and kidneys (CD45R<sup>+</sup>)

indicative of ELS, tissue morphometry was performed as described previously (52). Briefly, slides were digitized with a VS110 Virtual Slide System (Olympus). The entire tissue was selected as the region of interest and 20% of the sections were captured by systematic random sampling with NewCast software (Visiopharm, Hoersholm, Denmark) and a virtual magnification of 20X. Percentages of CD45R<sup>+</sup>, CD3<sup>+</sup>, or CD21/CD35<sup>+</sup> cells were calculated by projecting a point grid over randomly sampled images with the STEPanizer v 1.8 stereology tool (56) and tallying the number of points falling onto positive staining or reference tissue.

## Statistics

All treatments consisted of 8 mice per group, and data are presented as mean  $\pm$  SEM. One mouse in the 5 wk CON/VEH group died of unknown causes during the course of the experiment; it did not show the typical signs of sickness including loss of body weight before death. The Shapiro-Wilk test was used to determine if data were distributed normally, and the robust outlier (ROUT) test ( $Q = 1\%$ ) was used to identify putative outliers. For data sets that met assumptions for normality and equal variance, a two-way ANOVA was used with treatment and time point as the experimental factors. For data that were normally distributed but unequal in variance, a log<sub>10</sub> transformation was applied and the parametric two-way ANOVA was performed. Then, for each time point, the Sidak's *post-hoc* test for multiple comparisons was used for the following pairwise comparisons identified *a priori*: CON/VEH vs. CON/cSiO<sub>2</sub>; CON/cSiO<sub>2</sub> vs. Low DHA/cSiO<sub>2</sub>; and CON/cSiO<sub>2</sub> vs. High DHA/cSiO<sub>2</sub>. For data obtained at a single time point, a one-way ANOVA was performed with the same *post-hoc* pairwise comparisons. Because the vast majority of histopathology score data were not normally distributed and not suitable for typical data transformations, these data were analyzed using the nonparametric Kruskal-Wallis ANOVA on ranks (either two-way or one-way, depending on the data set) followed by Dunn's multiple comparisons tests for the pairwise tests outlined above. A  $p$  value  $< 0.05$  was considered statistically different for main effects of treatment, time point or treatment  $\times$  time point and for the pairwise comparisons to the negative (CON/VEH) or positive control (CON/cSiO<sub>2</sub>) for all study outcomes. Statistical analyses were performed using GraphPad Prism v.7 (La Jolla, CA).

## RESULTS

### DHA Is Incorporated in Tissues at the Expense of ARA

GLC analysis confirmed that projected FA content of experimental diets (Table 1) was consistent with their final compositions (Table 2). Erythrocytes were further analyzed to ascertain how experimental diets influenced tissue FA profiles (57). Consumption of DHA (C22:6  $\omega$ -3) resulted in increased erythrocyte concentrations of this FA and concurrently decreased ARA (C20:4  $\omega$ -6) at 1 wk PI (Table 3). Interestingly, although DHA was the predominant  $\omega$ -3 PUFA, EPA (C20:5  $\omega$ -3) accounted for 16 and 21 percent of total  $\omega$ -PUFAs in erythrocytes from mice fed the Low DHA and High DHA diets,

**TABLE 2 |** Fatty acid (FA) content of experimental diets.

	CON	Low DHA	High DHA
C12:0	0.04 $\pm$ 0.00	0.62 $\pm$ 0.00	1.42 $\pm$ 0.07
C14:0	0.16 $\pm$ 0.01	1.79 $\pm$ 0.02	4.15 $\pm$ 0.21
C15:0	0.03 $\pm$ 0.00	0.02 $\pm$ 0.00	0.03 $\pm$ 0.00
C16:0	5.64 $\pm$ 0.04	6.82 $\pm$ 0.02	7.79 $\pm$ 0.02
C16:1 7 c/8 c	0.03 $\pm$ 0.00	0.03 $\pm$ 0.00	0.03 $\pm$ 0.00
C16:1 9 c	0.08 $\pm$ 0.00	0.41 $\pm$ 0.00	0.86 $\pm$ 0.03
C17:0	0.03 $\pm$ 0.00	0.04 $\pm$ 0.00	0.04 $\pm$ 0.00
C18:0	1.71 $\pm$ 0.01	1.56 $\pm$ 0.01	1.39 $\pm$ 0.02
C18:1 9 c	71.08 $\pm$ 0.13	62.40 $\pm$ 0.08	53.26 $\pm$ 0.50
C18:1 11 c	0.75 $\pm$ 0.02	0.65 $\pm$ 0.01	0.55 $\pm$ 0.01
C18:2 ( $\omega$ -6)	19.17 $\pm$ 0.10	18.94 $\pm$ 0.01	15.08 $\pm$ 0.79
C20:0	0.31 $\pm$ 0.00	0.28 $\pm$ 0.00	0.24 $\pm$ 0.00
C18:3 ( $\omega$ -3)	0.36 $\pm$ 0.01	0.37 $\pm$ 0.00	0.32 $\pm$ 0.01
C22:0	0.22 $\pm$ 0.00	0.21 $\pm$ 0.00	0.20 $\pm$ 0.00
C24:0	0.14 $\pm$ 0.00	0.13 $\pm$ 0.00	0.12 $\pm$ 0.01
C22:5 ( $\omega$ -3)	0.00 $\pm$ 0.00	0.09 $\pm$ 0.00	0.20 $\pm$ 0.01
C22:6 ( $\omega$ -3)	0.00 $\pm$ 0.00	5.40 $\pm$ 0.05 <sup>a</sup>	14.20 $\pm$ 0.65 <sup>b</sup>
$\Sigma$ SFA	8.3 $\pm$ 0.1	11.5 $\pm$ 0.1	15.4 $\pm$ 0.1
$\Sigma$ MUFA	71.9 $\pm$ 0.1	63.5 $\pm$ 0.1	54.7 $\pm$ 0.5
$\Sigma$ PUFA ( $\omega$ -3)	0.4 $\pm$ 0.01	5.9 $\pm$ 0.1	14.7 $\pm$ 0.7
$\Sigma$ PUFA ( $\omega$ -6)	19.2 $\pm$ 0.1	18.9 $\pm$ 0.0	15.1 $\pm$ 0.8
$\omega$ -6: $\omega$ -3	52.8 $\pm$ 1.3	3.2 $\pm$ 0.0	1.0 $\pm$ 0.1

Data shown are mean percent of total lipid in diet  $\pm$  SEM or the ratio of  $\omega$ -6 to  $\omega$ -3 FAs of three representative diets as determined by GLC.

<sup>a</sup> Equivalent to 3.9 g/kg DHA diet.

<sup>b</sup> Equivalent to 9.9 g/kg DHA diet.

respectively. FA content in erythrocytes at 1 wk PI (Table 3) did not appreciably differ from that of the 5, 9, or 13 wk PI (Supplementary Tables 1–3). This suggested that  $\omega$ -3 PUFA incorporation peaked within 6 wk of initiating DHA feeding and remained stable throughout the course of the experiment.

### DHA Consumption Suppresses cSiO<sub>2</sub>-Induced Mononuclear Cell Elevation in BALF

Total cell counts in BALF of cSiO<sub>2</sub>-exposed mice fed CON diet were modestly increased at 1 and 5 wk PI compared to VEH-treated mice fed CON diet (Figure 2). By 9 and 13 wk PI, cell numbers in the CON/cSiO<sub>2</sub> group were dramatically elevated. Rank order of the inflammatory cell populations was macrophage  $>$  neutrophils  $>$  lymphocytes with eosinophils being negligibly affected. cSiO<sub>2</sub>-induced inflammatory cell recruitment in the lung alveolar space was suppressed significantly at 9 and 13 wk PI in mice consuming the Low DHA and High DHA diets (Figure 2, Supplementary Table 5).

### DHA Supplementation Blocks cSiO<sub>2</sub>-Induced Inflammation and Cell Infiltration in Lung

At 1 and 5 wk PI, small lesions were evident in the lungs of the CON/cSiO<sub>2</sub> group as compared to CON/VEH group

**TABLE 3** | Fatty acid (FA) content of erythrocytes at 1 wk post-instillation (PI).

	CON/ VEH	CON/ cSiO <sub>2</sub>	Low DHA/ cSiO <sub>2</sub>	High DHA/ cSiO <sub>2</sub>
C14:0	0.15 ± 0.01	0.15 ± 0.01	0.23 ± 0.03	0.29 ± 0.03
C16:0	24.79 ± 0.43	24.70 ± 0.45	27.13 ± 0.54	29.11 ± 0.48
C16:1n7t	0.04 ± 0.01	0.04 ± 0.01	0.03 ± 0.01	0.03 ± 0.01
C16:1n7	0.59 ± 0.08	0.64 ± 0.03	0.61 ± 0.61	0.63 ± 0.10
C18:0	16.04 ± 0.42	15.87 ± 0.22	15.07 ± 0.32	14.30 ± 0.48
C18:1t	0.16 ± 0.01	0.16 ± 0.01	0.15 ± 0.01	0.14 ± 0.01
C18:1 ω-9	17.28 ± 0.51	17.19 ± 0.26	15.77 ± 0.54	15.01 ± 0.14
C18:2 ω-6t	0.06 ± 0.01	0.07 ± 0.01	0.05 ± 0.00	0.05 ± 0.00
C18:2 ω-6	9.35 ± 0.058	9.24 ± 0.51	11.71 ± 0.45	11.15 ± 0.75
C20:0	0.16 ± 0.02	0.14 ± 0.02	0.16 ± 0.02	0.15 ± 0.01
C18:3 ω-6	0.06 ± 0.02	0.07 ± 0.01	0.05 ± 0.01	0.03 ± 0.00
C20:1n9	0.43 ± 0.02	0.39 ± 0.02	0.30 ± 0.03	0.23 ± 0.02
C18:3 ω-3	0.04 ± 0.00	0.04 ± 0.00	0.05 ± 0.01	0.04 ± 0.01
C20:2 ω-6	0.27 ± 0.02	0.27 ± 0.01	0.25 ± 0.03	0.17 ± 0.01
C22:0	0.12 ± 0.01	0.11 ± 0.03	0.13 ± 0.03	0.13 ± 0.02
C20:3 ω-6	1.36 ± 0.10	1.43 ± 0.07	1.35 ± 0.16	0.80 ± 0.06
C20:4 ω-6	19.56 ± 0.89	19.97 ± 0.56	8.46 ± 0.50	3.90 ± 0.22
C24:0	0.21 ± 0.03	0.22 ± 0.05	0.25 ± 0.05	0.29 ± 0.05
C20:5 ω-3	0.24 ± 0.04	0.30 ± 0.03	2.75 ± 0.33	4.80 ± 0.26
C24:1 ω-9	0.24 ± 0.04	0.23 ± 0.06	0.24 ± 0.05	0.23 ± 0.04
C22:4 ω-6	1.98 ± 0.15	1.88 ± 0.06	0.38 ± 0.04	0.16 ± 0.02
C22:5 ω-6	0.68 ± 0.04	0.65 ± 0.04	0.09 ± 0.02	0.05 ± 0.01
C22:5 ω-3	0.58 ± 0.05	0.61 ± 0.03	0.94 ± 0.04	0.91 ± 0.05
C22:6 ω-3	5.59 ± 0.36	5.62 ± 0.20	13.85 ± 0.42	17.40 ± 0.64
∑ SFA	41.47 ± 0.49	41.19 ± 0.44	42.97 ± 0.46	44.26 ± 0.53
∑ MUFA	18.74 ± 0.49	18.66 ± 0.26	17.10 ± 0.63	16.27 ± 0.15
∑ PUFA (ω-3)	6.45 ± 0.44	6.57 ± 0.21	17.58 ± 0.58	23.15 ± 0.84
∑ PUFA (ω-6)	33.34 ± 0.51	33.58 ± 0.41	22.35 ± 0.84	16.32 ± 0.82

Analysis of experimental groups from 1 wk after final cSiO<sub>2</sub> instillation. Data shown are mean percent of total FA ± SEM (n = 8 per group) as determined by GLC. Data for 5, 9, and 13 wk PI can be found in **Supplementary Tables 1–3**, respectively.

(**Figure 3A**, **Table 4**). Lymphoid aggregates in interstitial tissue circumventing the airways and blood vessels were present in some cSiO<sub>2</sub>-treated mice; mild alveolar proteinosis and alveolitis were similarly apparent. By 9 wk PI, pulmonary lesions in the CON/cSiO<sub>2</sub> group were more severe (**Figure 3C**, **Table 4**, **Supplementary Table 4**). ELS formation closely paralleled increases in lymphoid aggregates in CON/cSiO<sub>2</sub> mice. These features were predominately present as interstitial lymphocytic infiltrates encompassing the airways and blood vessels in the lungs. Consumption of the High DHA diet diminished the size of these lymphocytic lesions at 9 wk PI but did not appreciably impact development of alveolar proteinosis or type II alveolar epithelial cell hyperplasia.

Consistent with previous findings (35, 52), cSiO<sub>2</sub> triggered severe inflammation and ELS expansion at 13 wk PI (**Figures 3B,E**, **Table 4**). In addition, mucous cell metaplasia in the respiratory epithelium lining large-diameter bronchioles was observed that was not evident at earlier time points. Attenuation of lymphocyte-dependent lesions (i.e., lymphoid aggregates and ELS) was evident in both the Low DHA and High DHA groups (**Figures 3D,F**, **Table 4**, **Supplementary Table 4**). Consumption

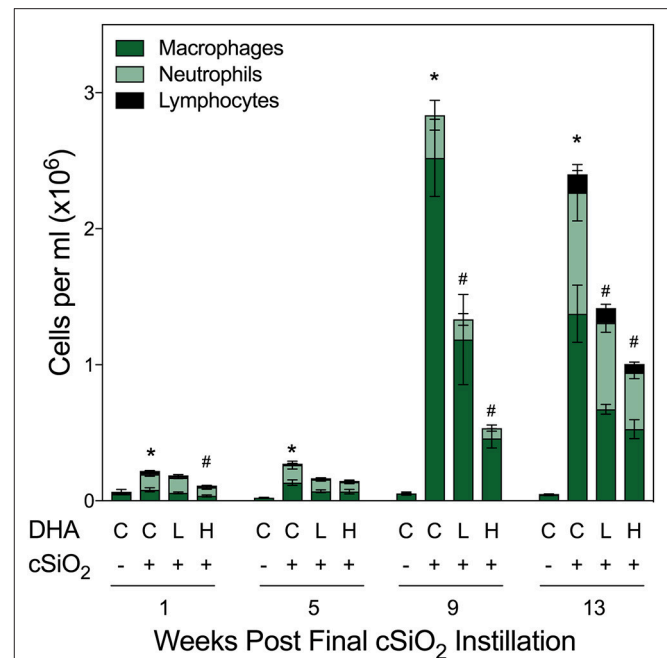


**FIGURE 2** | DHA supplementation suppresses cSiO<sub>2</sub>-induced elevation of inflammatory cells in BALF. Total cell counts in BALF samples from NZBWF1 mice were conducted using a hemocytometer and then monocytes/macrophages, lymphocytes, neutrophils, and eosinophils quantified after differential staining using morphological criteria. Abbreviations: C, control diet; L, Low DHA diet; H, High DHA diet. Data are means ± SEM (n = 7–8 per group). Symbols: \* indicates significantly different from CON/VEH group (p < 0.05); # indicates significantly different from CON/cSiO<sub>2</sub> group (p < 0.05). Complete statistical analyses can be found in **Supplementary Table 5**.

of the High DHA diet reduced cSiO<sub>2</sub>-induced alveolitis at this time point, but this response was not evident in mice fed the Low DHA diet. However, DHA did not markedly impact cSiO<sub>2</sub>-induced lymphocyte-independent histopathological lesions including alveolar proteinosis, type II alveolar epithelial cell hyperplasia, and mucous cell metaplasia.

## Dietary DHA Delays cSiO<sub>2</sub>-Induced Accumulation of B- and T-Cell Aggregates in Lung Over Time

Morphometry was used on immunohistochemically stained slides from the lung to (1) quantify changes in B- and T-cells during cSiO<sub>2</sub>-induced pulmonary ectopic lymphoid neogenesis and (2) assess DHA's influence on these lymphocyte populations over time. cSiO<sub>2</sub> elicited early and sustained CD45R<sup>+</sup> B-cell and CD3<sup>+</sup> T-cell elevation in lungs of mice fed CON diet at 1 and 5 wk PI (**Figures 4A,G**, **5A,G**). B- and T- cells occurred mostly within diffuse interstitial infiltrates and did not appear to organize into distinct ELS at these time points. By 9 wk PI, cSiO<sub>2</sub> instillation caused pronounced formation of focal B-cell aggregates interspersed with more diffuse T-cells in CON-fed mice, thus resembling ELS with functional germinal centers (**Figures 4C,G**, **5C,G**). ELS in CON/cSiO<sub>2</sub> group were dramatically expanded by 13 wk PI (**Figures 4E,G**, **5E,G**)

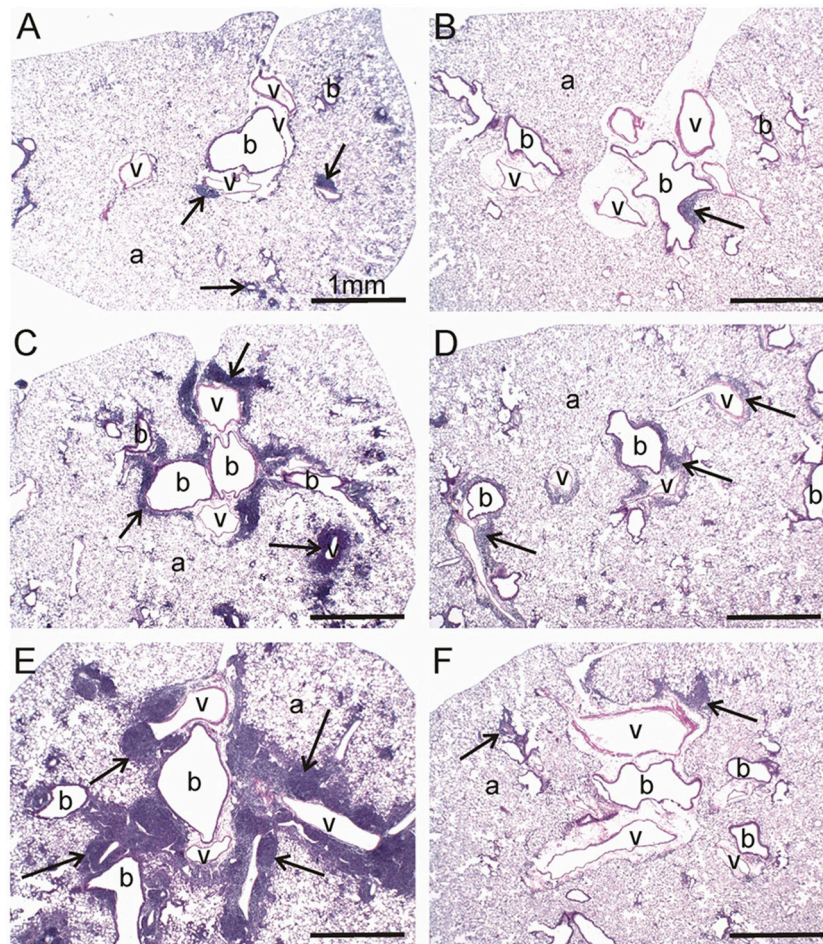


**FIGURE 3 |** DHA consumption prevents cSiO<sub>2</sub>-triggered inflammation in lungs of NZBWF1 mice. Representative light photomicrographs depict H&E-stained lung sections from CON/cSiO<sub>2</sub> groups at (A) 5 wk post-instillation (PI), (C) 9 wk PI, and (E) 13 wk PI; (B) CON/VEH at 13 wk PI; (D) Low DHA/cSiO<sub>2</sub> at 13 wk PI; and (F) High DHA/cSiO<sub>2</sub> at 13 wk PI. Black arrows in photomicrographs indicate lymphoid cell infiltration in the peribronchiolar and perivascular interstitium. Dietary DHA substantially suppressed lymphocytic infiltration (D, F; See also Table 4). Abbreviations: a, alveolar parenchyma; b, bronchiolar airway; v, blood vessel.

compared to VEH-treated mice fed control diet (Figures 4B, 5B). Notably, consumption of either Low DHA and High DHA diets was markedly effective at restricting cSiO<sub>2</sub>-induced B- and T-cell accumulation across all experimental time points (Figures 4D,E,G, 5D,E,G, Supplementary Table 5).

### DHA Supplementation Impedes cSiO<sub>2</sub>-Induced Formation Ectopic Germinal Centers

Immunohistochemistry for CD21<sup>+</sup>/CD35<sup>+</sup> was used to quantify FDCs, markers of germinal centers, in ELS of CON/cSiO<sub>2</sub> mice. FDC numbers were not affected by cSiO<sub>2</sub> in lung sections from 1 or 5 wk PI (Figures 6A,G). However, by 9 and 13 wk PI, there was marked infiltration and networking of FDCs in CON/cSiO<sub>2</sub> groups (Figures 6C,E,G) compared to corresponding CON/VEH mice (Figures 6B,G). FDCs were found predominately in the perivascular and peribronchial regions, which was consistent with the location of CD45R<sup>+</sup>

and CD3<sup>+</sup> cell infiltrates. Remarkably, cSiO<sub>2</sub>-induced FDC accumulation was nearly completely ablated in mice consuming either DHA diets (Figures 6D,F,G, Supplementary Table 5). In concert with FDC findings, large aggregates (Figure 7B) of IgG<sup>+</sup> plasma cells were present in the pulmonary perivascular and peribronchiolar interstitial tissue and were associated with ectopic lymphoid structures in CON/cSiO<sub>2</sub> mice at wk 13. These were significantly diminished in the mice fed low and high DHA diets (Figures 7C,D,E). IgG<sup>+</sup> plasma cells were few and widely scattered in these regions of lung in CON/VEH mice (Figures 7A,E). Accordingly, cSiO<sub>2</sub> exposure elicited ectopic lymphoid germinal center development, but this response was blocked by inclusion of DHA in the diet.

### DHA Suppresses Induction of Plasma Anti-dsDNA Autoantibodies by cSiO<sub>2</sub>

Robust anti-dsDNA IgG responses were observed in BALF (Figure 7F) and plasma (Figure 8, Supplementary Table 5) of

**TABLE 4** | Histopathological assessment of cSiO<sub>2</sub>-triggered pulmonary inflammation in female NZBWF1 mice fed CON or DHA-enriched diets at 1, 5, 9, and 13 wk post-instillation.

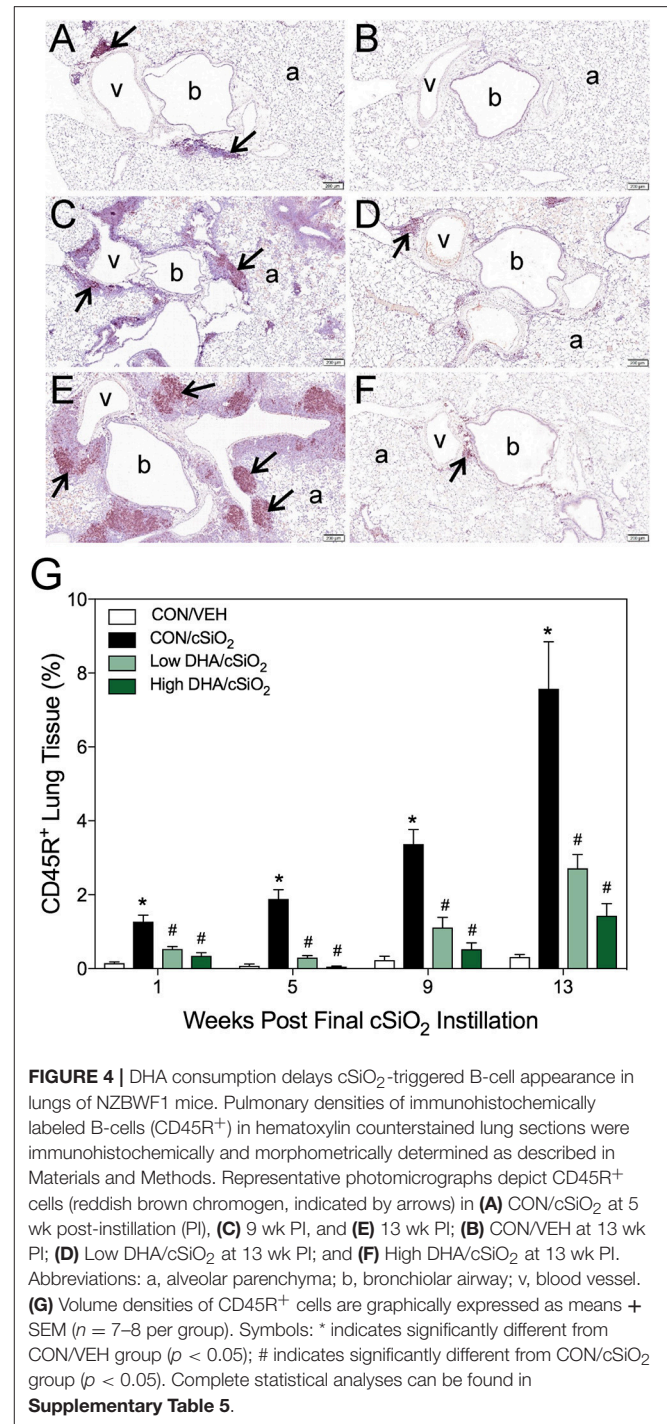
	Week	CON/ VEH	CON/ cSiO <sub>2</sub>	Low DHA/ cSiO <sub>2</sub>	High DHA/ cSiO <sub>2</sub>
Lymphoid aggregates	1	0.6 ± 0.2	1.1 ± 0.1	0.9 ± 0.1	0.8 ± 0.2
	5	0.6 ± 0.2	1.5 ± 0.2*	1.1 ± 0.1	0.8 ± 0.1
	9	1.0 ± 0.0	3.1 ± 0.2*	2.2 ± 0.1	1.1 ± 0.2#
	13	0.9 ± 0.1	3.6 ± 0.2*	2.0 ± 0.2#	1.6 ± 0.2#
Ectopic lymphoid structures	1	0.0 ± 0.0	0.2 ± 0.2	0.0 ± 0.0	0.0 ± 0.0
	5	0.0 ± 0.0	0.1 ± 0.1	0.0 ± 0.0	0.0 ± 0.0
	9	0.4 ± 0.0	2.4 ± 0.2*	1.2 ± 0.2	0.6 ± 0.2#
	13	0.0 ± 0.0	3.4 ± 0.2*	1.6 ± 0.3	1.1 ± 0.3#
Alveolar proteinosis	1	0.0 ± 0.0	1.5 ± 0.3*	1.1 ± 0.1	1.0 ± 0.0
	5	0.0 ± 0.0	2.2 ± 0.2*	2.2 ± 0.2	2.1 ± 0.1
	9	0.0 ± 0.0	4.0 ± 0.2*	4.0 ± 0.0	4.0 ± 0.0
	13	0.0 ± 0.0	4.0 ± 0.1*	4.1 ± 0.1	4.1 ± 0.1
Alveolitis	1	0.0 ± 0.0	1.0 ± 0.0*	1.0 ± 0.0	0.4 ± 0.1#
	5	0.0 ± 0.0	1.2 ± 0.2*	1.0 ± 0.0	1.0 ± 0.0
	9	0.0 ± 0.0	2.6 ± 0.3*	1.9 ± 0.2	1.1 ± 0.2#
	13	0.0 ± 0.0	2.8 ± 0.2*	2.2 ± 0.2	2.0 ± 0.2
Type II alveolar epithelial cell hyperplasia	1	0.0 ± 0.0	0.0 ± 0.0	0.0 ± 0.0	0.0 ± 0.0
	5	0.0 ± 0.0	0.0 ± 0.0	0.0 ± 0.0	0.0 ± 0.0
	9	0.0 ± 0.0	0.6 ± 0.2*	0.6 ± 0.2	0.6 ± 0.2
	13	0.0 ± 0.0	2.2 ± 0.2*	1.6 ± 0.3	1.6 ± 0.3
Mucous cell metaplasia	1	0.0 ± 0.0	0.0 ± 0.0	0.0 ± 0.0	0.0 ± 0.0
	5	0.0 ± 0.0	0.0 ± 0.0	0.0 ± 0.0	0.0 ± 0.0
	9	0.0 ± 0.0	0.0 ± 0.0	0.0 ± 0.0	0.0 ± 0.0
	13	0.0 ± 0.0	2.2 ± 0.2	0.4 ± 0.2	0.1 ± 0.1

NZBWF1 mice ( $n = 7-8/\text{group}$ ) were graded individually for severity of lung inflammation (% of total pulmonary tissue) as follows: 0, no changes; 1, minimal (<10%); 2, slight (10–25%); 3, moderate (26–50%); 4, severe (51–75%); 5, very severe (> 75%) of total area affected. Data are shown as mean ± SEM score for each pathological lesion. \* indicates treatment group is significantly different compared to CON/VEH ( $p < 0.05$ ). # indicates treatment group is significantly different compared to CON/cSiO<sub>2</sub> ( $p < 0.05$ ). Complete statistical results are provided in **Supplementary Table 4**.

cSiO<sub>2</sub>-instilled mice fed CON diet at 9 and 13 week PI compared to VEH-treated mice fed CON diet. Consumption of DHA suppressed these autoantibody responses. Thus, cSiO<sub>2</sub>-induced anti-dsDNA IgG responses in BALF and plasma and their suppression by DHA recapitulated the impact of these agents on ectopic germinal center development in the lung.

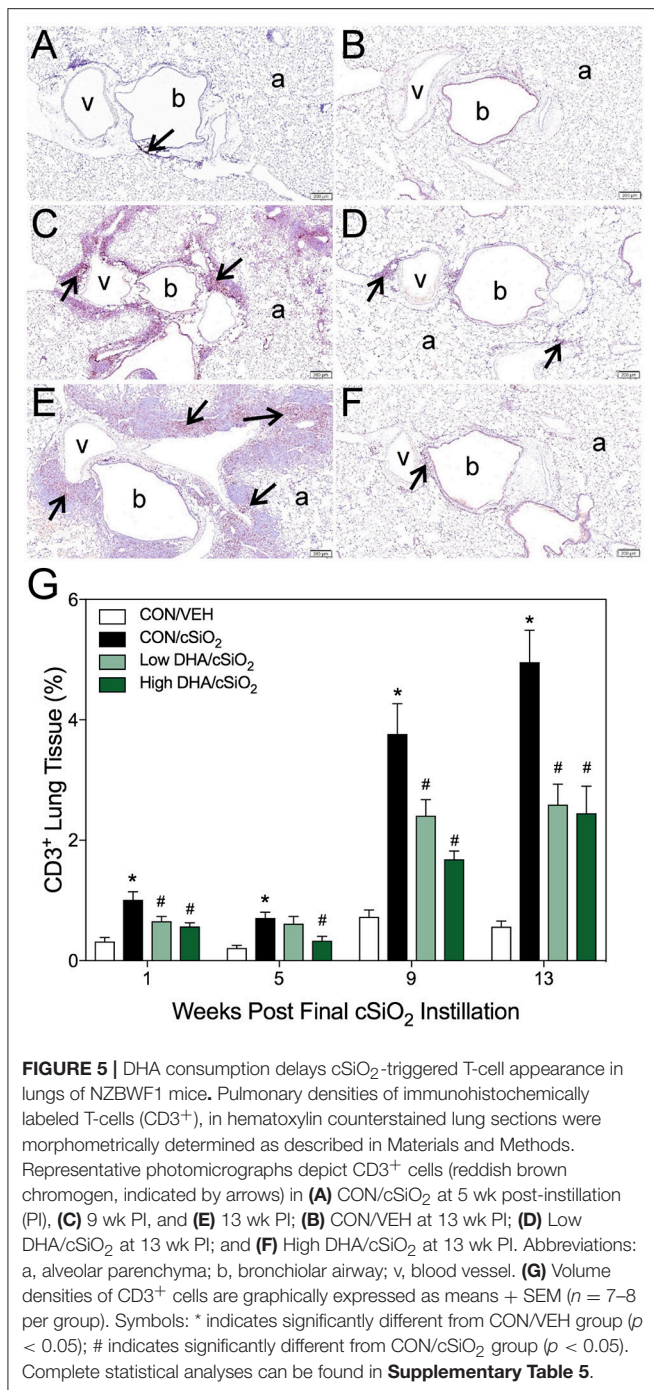
## Dietary DHA Diminishes cSiO<sub>2</sub>-Induced Glomerulonephritis and B-Cell Infiltration in the Kidney

Kidneys were evaluated histologically for glomerulonephritis over the entire experimental time course. Significant lesions were apparent only at 13 wk PI with nephritis being detectable

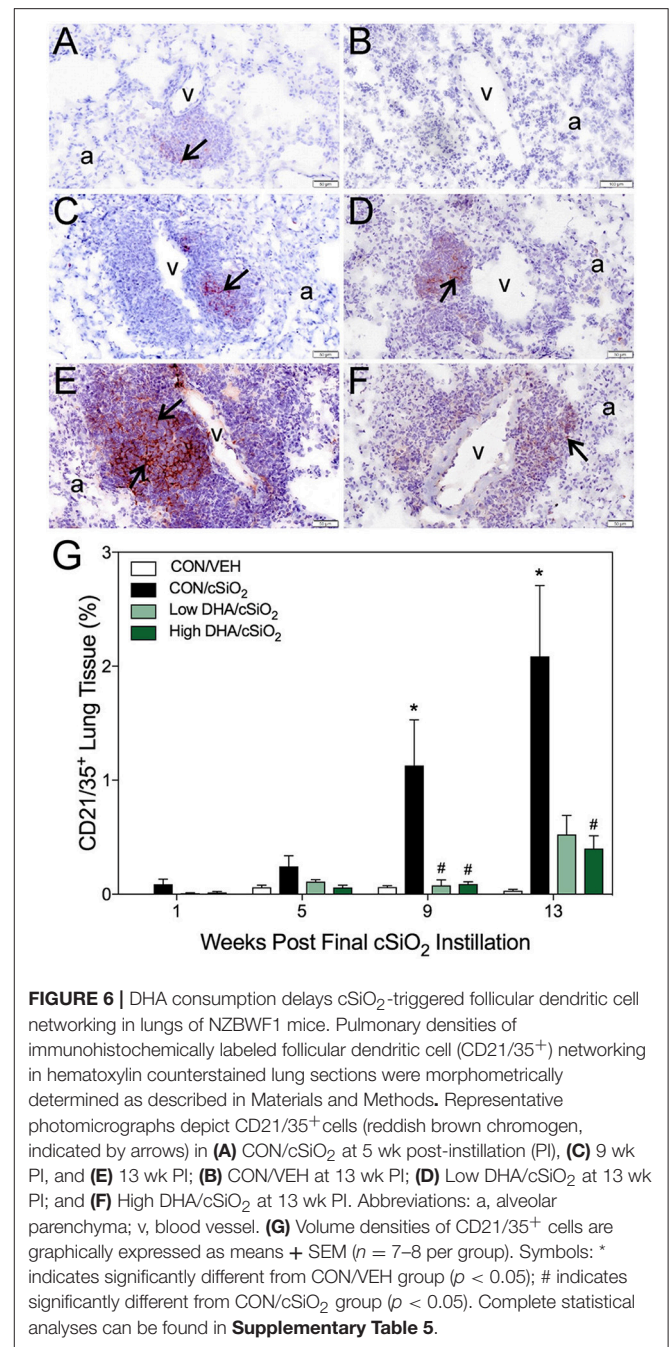


in 0, 5, 1, or 0 mice per group ( $n = 8$ ) in the CON/VEH, CON/cSiO<sub>2</sub>, Low DHA/cSiO<sub>2</sub>, or High DHA/cSiO<sub>2</sub> groups, respectively (Figures 9A–D). Tubular proteinosis was evident at 13 wk PI in the CON/cSiO<sub>2</sub> group but not in the CON/VEH, Low DHA/cSiO<sub>2</sub>, or High DHA/cSiO<sub>2</sub> groups (Figure 9E).

B-cell infiltrates in the kidney have been previously associated with severity of lupus nephritis (58–60). Marked cell infiltration was evident in kidney tissues of mice in the CON/cSiO<sub>2</sub>



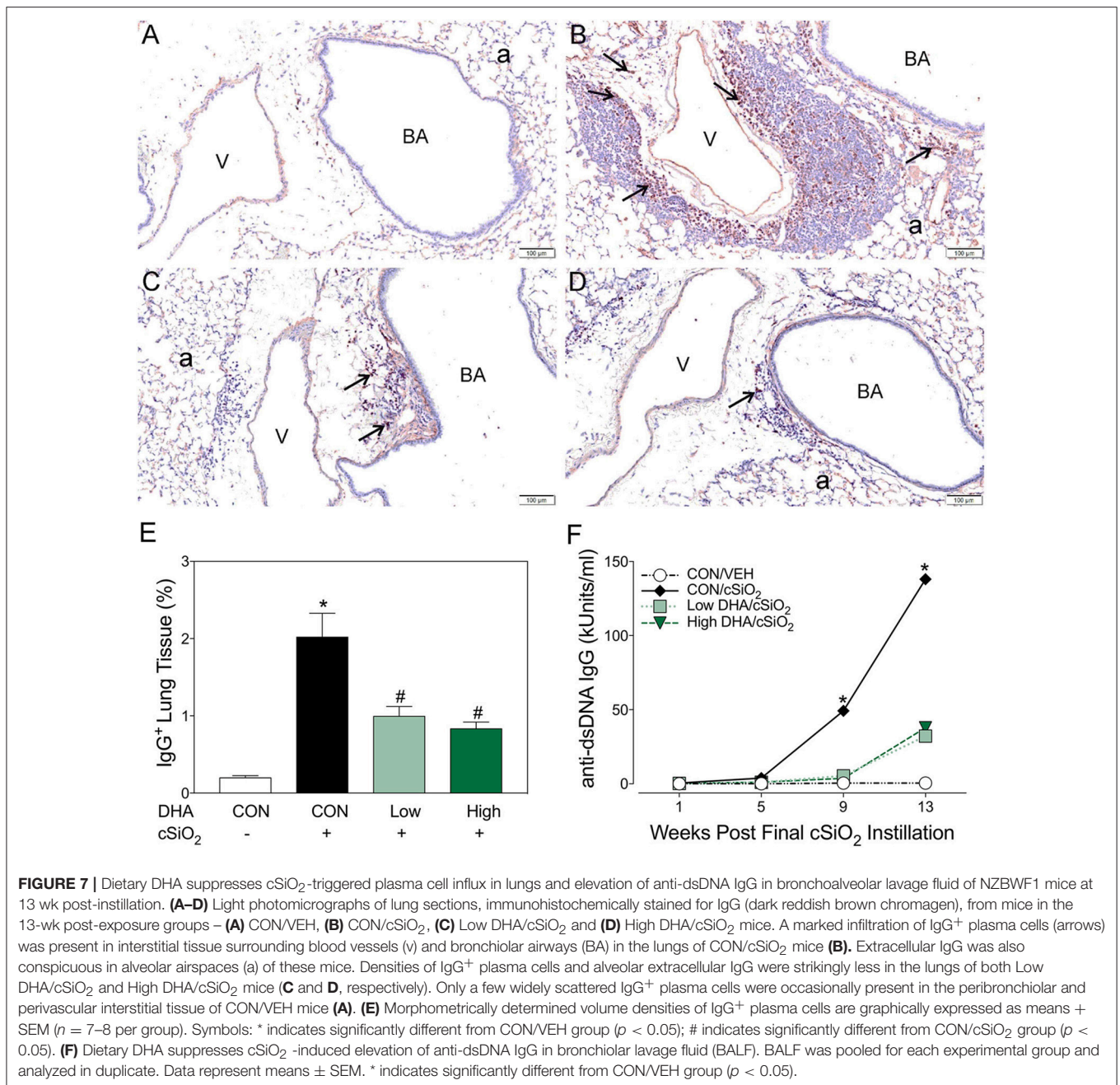
group at 13 wk PI compared to the other experimental groups. (Figures 10A–D). Immunohistochemistry revealed that in CON/cSiO<sub>2</sub> mice kidneys, CD45R<sup>+</sup> cells localized into distinct, focal aggregates in the interstitium surrounding interlobular arteries and veins in the renal cortex and near the renal pelvis (Figures 10E,F). A trend toward reduced cSiO<sub>2</sub>-triggered B-cell accumulation was evident in mice fed DHA (Figures 10G,H,I). Given that cSiO<sub>2</sub> particles in this study are too large to diffuse into systemic circulation via the lung and are



insoluble in water, it seems unlikely that these particles could be deposited in tissues distal to the lung. We did not observe cSiO<sub>2</sub> particles in kidney by birefringent microscopy (unpublished observations) suggesting the improbability of direct deposition of cSiO<sub>2</sub> particles in the kidney promoting CD45R<sup>+</sup> B-cell infiltration.

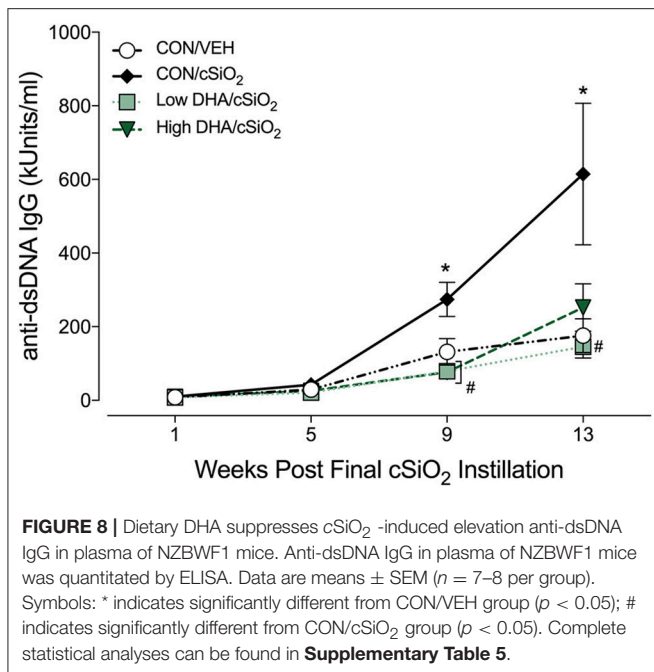
## DISCUSSION

Understanding how cSiO<sub>2</sub> triggers autoimmunity in this preclinical model is important not only because exposure to



this respirable particle has been linked to human autoimmune disease but also because this response serves as a model for agents that cause sterile inflammation. Inhalation of cSiO<sub>2</sub> elicits a cascade that includes: (1) phagocytosis by alveolar macrophages, (2) lysosomal membrane permeabilization, (3) inflammasome activation, (4) release of inflammatory mediators, and (5) cell death and release of free cSiO<sub>2</sub> particles (61–68). Since cSiO<sub>2</sub> clearance from the lung is minimal (69), persistent repetition of this cascade evokes buildup of cell corpses, secondary necrosis, alarmin release, and self-antigen presentation that very likely culminate in early loss of

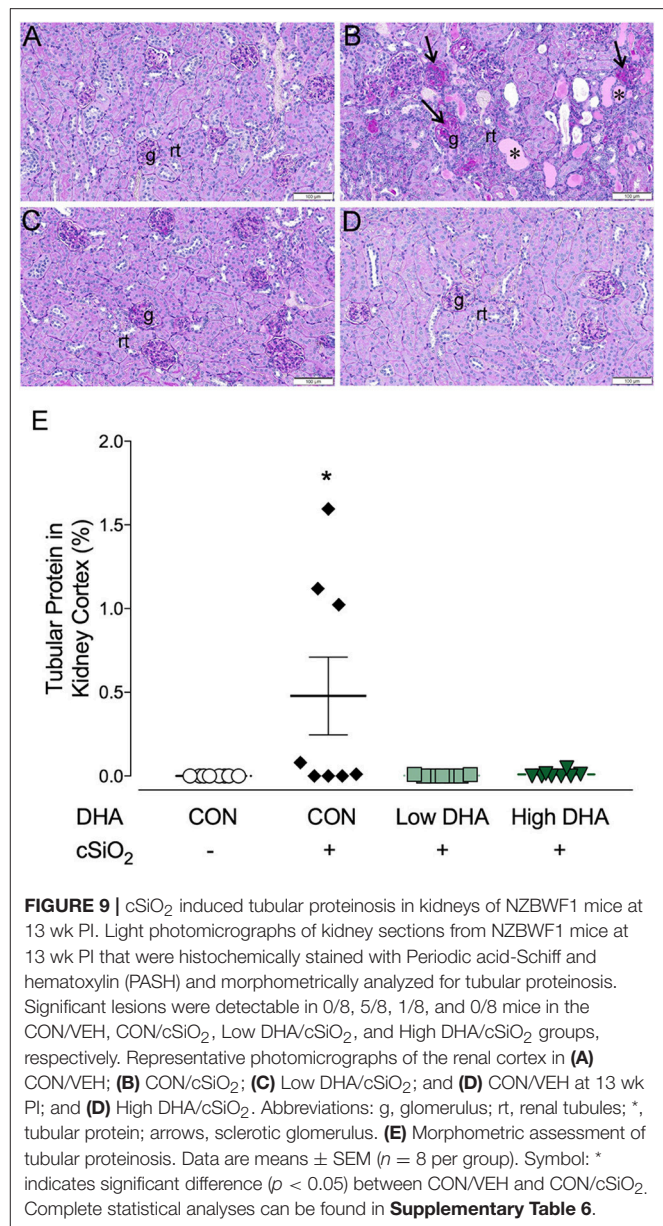
tolerance and autoimmunity. Consistent with this scenario, we report here for the first time that cSiO<sub>2</sub> instillation sequentially induces the accumulation of pulmonary B- and T-cell aggregates (1, 5 wk PI) → FDC networking and plasma cell accumulation in lung indicative of ectopic lymphoid germinal centers (9, 13 wk PI) → BALF and plasma anti-dsDNA IgG elevation (9, 13 wk PI) → glomerulonephritis with B-cell accumulation (13 wk PI). These observations provide unique insight into how respirable cSiO<sub>2</sub> might induce initiation and potentially flaring in lupus and other human ADs.



While our data suggest that the lung is likely to be a rich source of anti-dsDNA antibodies in the plasma, it is also possible that these could also originate at other sites such as the spleen as a result of lymphocyte homing from the lung or stimulation of new germinal centers by IgG-immune complexes arising from the lung. However, we did not detect histological differences in splenic architecture in the 13 wk cohort that would be suggestive of changes in germinal center development between CON/VEH and CON/cSiO<sub>2</sub> mice (data not shown).

Managing lupus involves reducing disease symptoms in newly diagnosed individuals and preventing progression of established tissue damage to organs such as kidney (70). Existing and emerging lupus therapies have multiple mechanisms of action, broadly encompassing non-specific immunosuppression, lymphocyte depletion, and neutralization of immune-stimulating cytokines and chemokines (70–73). These approaches have serious limitations including serious adverse effects, inability to reverse immune-mediated damage, and high costs (70, 74). Significantly, several studies have indicated that ELS function as a survival niches, potentially shielding autoreactive plasma cells from immunosuppressive therapies (75–77). Therefore, strategies are needed to block ELS development and limit their capacity to exacerbate lupus progression and severity.

Consumption of  $\omega$ -3 PUFAs such as DHA represents an alternative and/or complementary approach to mitigate autoimmune disease and other chronic health conditions. Omega-3 PUFAs are the most widely consumed nutritional supplement after multivitamins, taken by ~30 million Americans (78, 79). Dietary  $\omega$ -3 PUFA incorporation occurs in tissues and cells throughout the body, including immune cells. In general,  $\omega$ -3 PUFAs are considered anti-inflammatory and

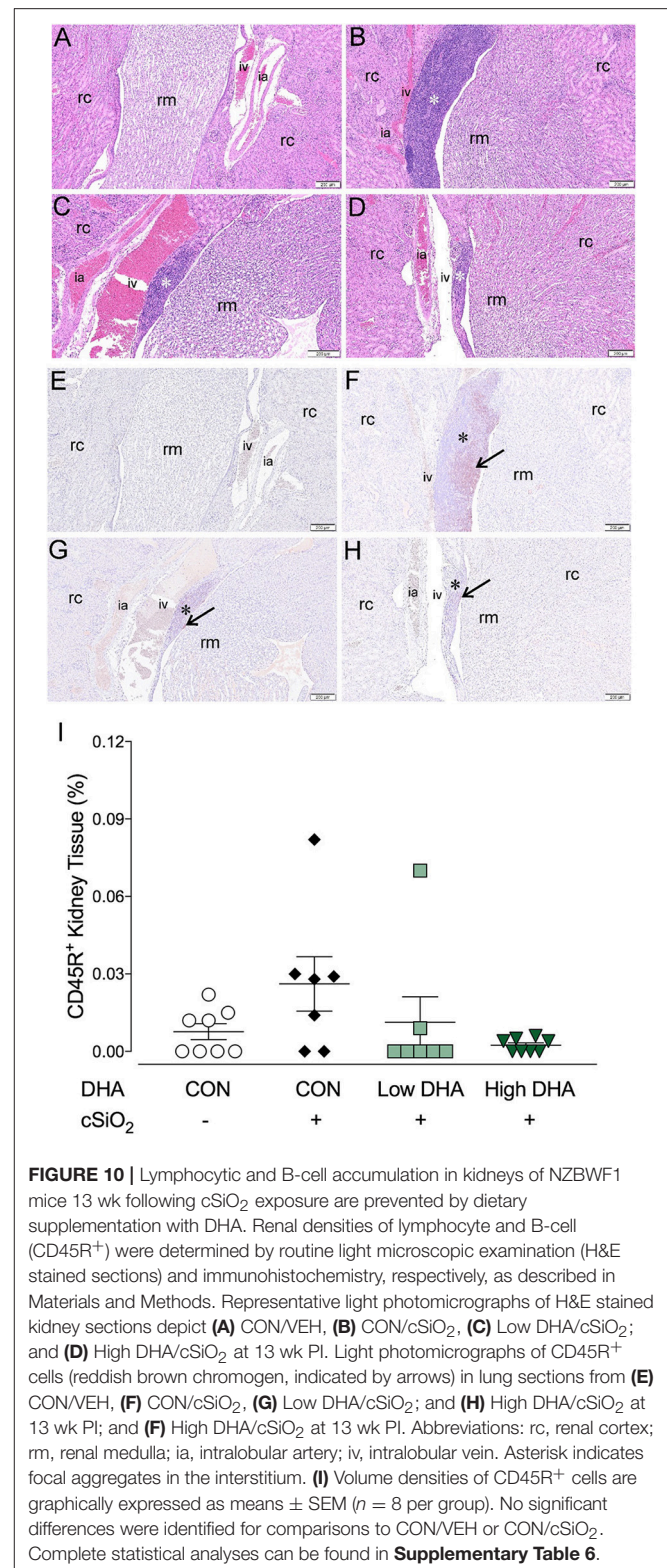


promote resolution of inflammation, whereas  $\omega$ -6 PUFAs are considered proinflammatory. Using FA content of erythrocytes, an established predictor of PUFA levels of other tissues in the body (57), we found here that dietary supplementation with DHA promoted incorporation of both DHA and another  $\omega$ -3 PUFA, EPA, at the expense of the  $\omega$ -6 PUFA ARA. Since the EPA content of the DHA diets was negligible, our findings suggest that there was enzymatic retroconversion of DHA to EPA as has been reported previously in mice fed DHA (80). A highly likely effect of increased  $\omega$ -3 PUFA tissue content is skewing of immune cells toward less inflammatory phenotypes that dampen chronic inflammation and autoimmunity (81). In support of that contention, we show here that dietary DHA supplementation, at levels that

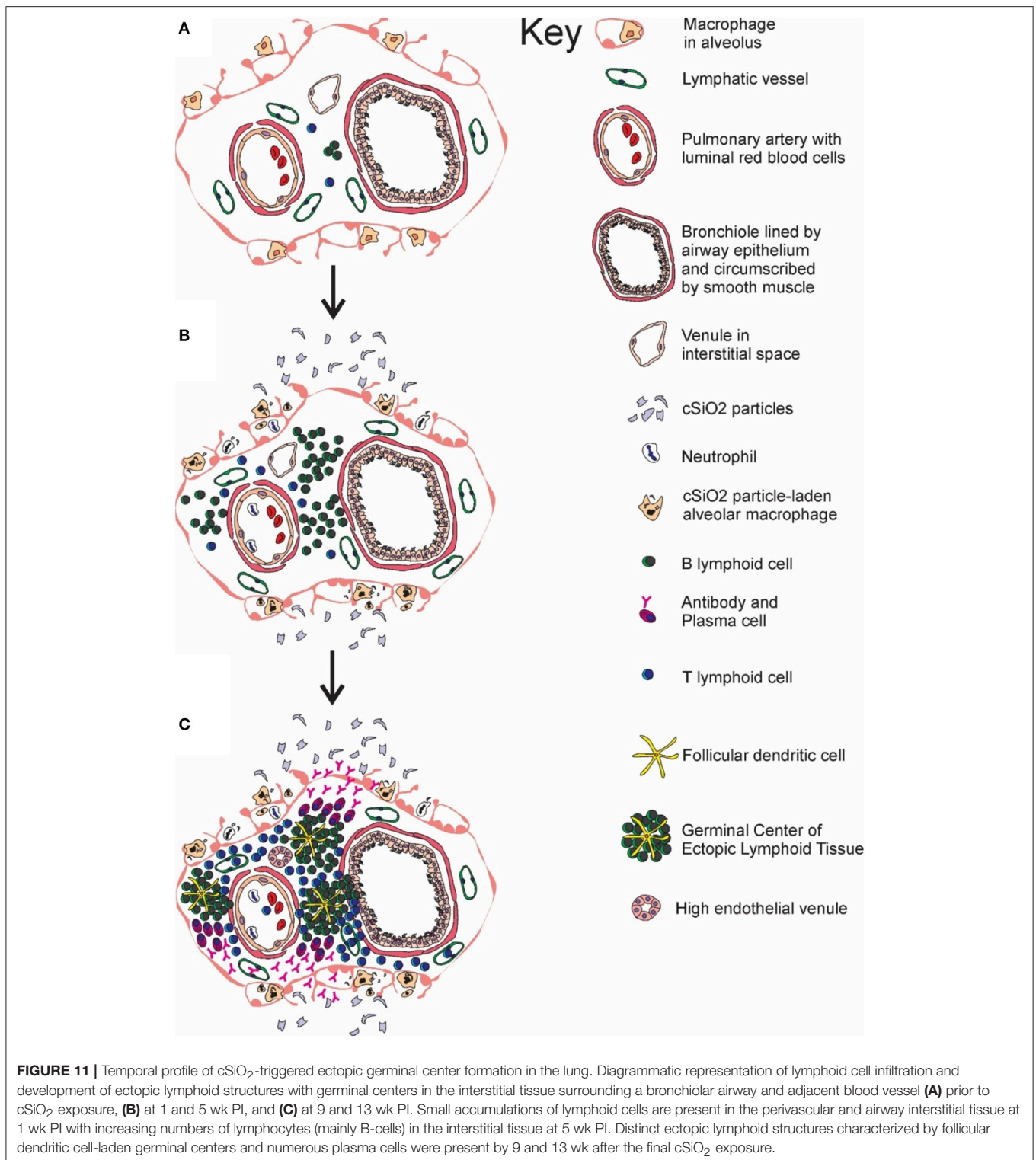
mimic realistic human consumption, blocked or delayed (1) pulmonary B-cell, T-cell, and FDC networking; (2) plasma autoantibody increases; and (3) glomerulonephritis and B-cell infiltration in the kidneys of cSiO<sub>2</sub>-treated mice. Accordingly, our findings are consistent with the possibility that  $\omega$ -3 PUFA supplementation might be practical strategy to intervene against an established environmental trigger of autoimmunity.

DHA and its retroconversion product EPA potentially quell cSiO<sub>2</sub>-triggered autoimmunity by altering bioactive lipid mediator production, intracellular signaling, transcription factor activity, gene expression, and membrane structure and function [reviewed in (40)]. Relative to bioactive lipid mediators, eicosanoids are a diverse category of metabolites that collectively include lipoxins, prostaglandins, and thromboxanes; these metabolites can influence both progression and resolution of inflammation. Eicosanoids are known to be induced in macrophages by cSiO<sub>2</sub> (82–86) and are associated with human lupus. These bioregulators are derived from metabolism of free (non-esterified) FAs that are liberated from the plasma membrane by activated phospholipase A2 (PLA<sub>2</sub>). The free FAs serve as substrates for cyclooxygenase, lipoxygenase, or cytochrome P450 enzymes. Competition for these enzymes by liberated PUFAs results in different metabolite signatures that can potentiate or attenuate inflammation. Generally, metabolites derived from  $\omega$ -6s like LA and ARA are considered proinflammatory, whereas  $\omega$ -3s produce specialized pro-resolving metabolites (SPMs) that enhance resolution of tissue inflammation (87). DHA-derived SPMs include the D-series resolvins, protectins, and maresins. Of special relevance to the cSiO<sub>2</sub> model, DHA and its SPMs have been shown to suppress inflammasome activation, prevent cell death, and enhance removal of cell corpses by efferocytosis (88–91). Toward this end, we are now focusing on how DHA and/or its SPMs influence alveolar macrophages responses to cSiO<sub>2</sub> and how these events shape autoimmunity.

Taken together, the results presented herein demonstrate that cSiO<sub>2</sub> instillation in a lupus-prone mouse model sequentially induced *de novo* ectopic lymphoid germinal center formation in the lung (depicted in **Figure 11**), systemic autoantibody elevation, and glomerulonephritis. Furthermore, all of these responses were inhibited by inclusion of DHA in the diet. Upon considering the potential adverse outcomes of DHA and other  $\omega$ -3 PUFAs, including those related to immune function, an expert committee of the European Food Safety Authority concluded that human intake up to 5 g/day is safe (92). Thus, the amounts of DHA used in this preclinical study, equivalent to 2 and 5 g/day human consumption, are consistent with realistic and safe doses in a clinical setting. Relative to human lupus, DHA supplementation may potentially aid two broad groups. One group is patients that are diagnosed with early-stage lupus where it could be used as a low-cost treatment, alone or as a complimentary approach to existing therapies. The second is individuals at increased risk for lupus who would benefit from a preventative measure with minimal side effects. This latter group could include asymptomatic



individuals who have a close family member with lupus or workers occupationally exposed to respirable silica or related particles. Future preclinical studies using the cSiO<sub>2</sub>-triggered



lupus-prone mouse models should focus on assessing the potential of DHA to serve as a therapeutic against established lupus and comparing the efficacy of DHA to established immunosuppressive agents used as the standard of care for individuals.

## DATA AVAILABILITY

The raw data supporting the conclusions of this manuscript will be made available by the authors, without undue reservation, to any qualified researcher.

## AUTHOR CONTRIBUTIONS

MB: study design, animal study coordination, silica exposures, necropsy, sample handling, ELISA, immunohistochemistry, morphometry, data analyses, and drafting the manuscript; PA: study design, immunohistochemistry, morphometry, data analyses, and manuscript preparation; KG: animal study coordination, diet preparation, mouse feeding, silica exposures, sample handling, data analyses, manuscript preparation; AK: methods development, morphometry, data analyses; DJ-H, JW, and NL: coordination and conduct of necropsies, cytology, morphometry, histopathology; KW: sample analysis, data interpretation, manuscript preparation; CB: study design, methods development; AH: experimental design, data interpretation, manuscript writing, project funding; AB: data analysis, manuscript preparation; JH: study design, lung/kidney histopathology, morphometry, data analyses, manuscript preparation, project funding; JP: planning, coordination, oversight, manuscript preparation/submission, project funding.

## REFERENCES

- Pons-Estel GJ, Ugarte-Gil MF, Alarcón GS. Epidemiology of systemic lupus erythematosus. *Exp Rev Clin Immunol*. (2017) 13:799–814. doi: 10.1080/1744666X.2017.1327352
- Stojan G, Petri M. Epidemiology of systemic lupus erythematosus: an update. *Curr Opin Rheumatol*. (2018) 30:144–50. doi: 10.1097/BOR.0000000000000480
- Moulton VR, Suarez-Fueyo A, Meidan E, Li H, Mizui M, Tsokos GC. Pathogenesis of human systemic lupus erythematosus: a cellular perspective. *Trends Mol Med*. (2017) 23:615–35. doi: 10.1016/j.molmed.2017.05.006
- Flores-Mendoza G, Sanson SP, Rodriguez-Castro S, Crispin JC, Rosetti F. Mechanisms of tissue injury in lupus nephritis. *Trends Mol Med*. (2018) 24:364–78. doi: 10.1016/j.molmed.2018.02.003
- Nacionales DC, Weinstein JS, Yan X-J, Albesiano E, Lee PY, Kelly-Scumpia KM, et al. B cell proliferation, somatic hypermutation, class switch recombination, and autoantibody production in ectopic lymphoid tissue in murine lupus. *J Immunol*. (2009) 182:4226–36. doi: 10.4049/jimmunol.0800771
- Weinstein JS, Nacionales DC, Lee PY, Kelly-Scumpia KM, Yan X-J, Scumpia PO, et al. Colocalization of antigen-specific B and T cells within ectopic lymphoid tissue following immunization with exogenous antigen. *J Immunol*. (2008) 181:3259–67. doi: 10.4049/jimmunol.181.5.3259
- Jones GW, Jones SA. Ectopic lymphoid follicles: inducible centres for generating antigen-specific immune responses within tissues. *Immunology* (2016) 147:141–51. doi: 10.1111/imm.12554
- McCloskey ML, Curotto de Lafaille MA, Carroll MC, Erlebacher A. Acquisition and presentation of follicular dendritic cell-bound antigen by lymph node-resident dendritic cells. *J Exp Med*. (2011) 208:135–48. doi: 10.1084/jem.20100354
- Kosco MH, Pflugfelder E, Gray D. Follicular dendritic cell-dependent adhesion and proliferation of B cells *in vitro*. *J Immunol* (1992) 148:2331–9.
- He DN, Chen WL, Long KX, Zhang X, Dong GF. Association of serum CXCL13 with intrarenal ectopic lymphoid tissue formation in lupus nephritis. *J Immunol Res*. (2016) 2016:e4832543. doi: 10.1155/2016/4832543
- Magliozzi R, Howell O, Vora A, Serafini B, Nicholas R, Puopolo M, et al. Meningeal B-cell follicles in secondary progressive multiple sclerosis associate with early onset of disease and severe cortical pathology. *Brain J Neurol*. (2007) 130:1089–104. doi: 10.1093/brain/awm038
- Amft N, Curnow SJ, Scheel-Toellner D, Devadas A, Oates J, Crocker J, et al. Ectopic expression of the B cell-attracting chemokine BCA-1 (CXCL13) on endothelial cells and within lymphoid follicles contributes

## FUNDING

Research was funded by NIH ES027353 (JP, JH, AH), NIH T32ES007255 (KW), Lupus Foundation of America (MB, JP), and the Dr. Robert and Carol Deibel Family Endowment (JP).

## ACKNOWLEDGMENTS

We would like to thank Amy Freeland, Lysie Eldridge, Adam Lock, and Ryan Lewandowski for their excellent technical advice and support, and Amy Porter and Kathy Joseph from the Michigan State University Histopathology Laboratory.

## SUPPLEMENTARY MATERIAL

The Supplementary Material for this article can be found online at: <https://www.frontiersin.org/articles/10.3389/fimmu.2018.02002/full#supplementary-material>

- to the establishment of germinal center-like structures in Sjögren's syndrome. *Arthritis Rheum*. (2001) 44:2633–41. doi: 10.1002/1529-0131(200111)44:11<2633::AID-ART443>3.0.CO;2-9
- Grewal JS, Pilgrim MJ, Grewal S, Kasman L, Werner P, Bruornton ME, et al. Salivary glands act as mucosal inductive sites via the formation of ectopic germinal centers after site-restricted MCMV infection. *FASEB J*. (2011) 25:1680–96. doi: 10.1096/fj.10-174656
- Dong W, Li X, Liu H, Zhu P. Infiltrations of plasma cells in synovium are highly associated with synovial fluid levels of APRIL in inflamed peripheral joints of rheumatoid arthritis. *Rheumatol Int*. (2009) 29:801–6. doi: 10.1007/s00296-008-0773-7
- Gulati G, Brunner HI. Environmental triggers in systemic lupus erythematosus. *Sem Arthritis Rheum*. (2017) 47:710–7. doi: 10.1016/j.semarthrit.2017.10.001
- NIAID Autoimmune Diseases Coordinating Committee. *Progress in Autoimmune Diseases Research*. NIAID Report to Congress [Internet]. (2005). Available online at: <https://www.niaid.nih.gov/topics/autoimmune/Documents/adccfinal.pdf>
- Parks CG, de Souza Espindola Santos A, Barbhuiya M, Costenbader KH. Understanding the role of environmental factors in the development of systemic lupus erythematosus. *Best Pract Res Clin Rheumatol*. (2017) 31:306–20. doi: 10.1016/j.berh.2017.09.005
- Perl A. Review: metabolic control of immune system activation in rheumatic diseases. *Arthritis Rheumatol*. (2017) 69:2259–70. doi: 10.1002/art.40223
- Miller FW, Alfredsson L, Costenbader KH, Kamen DL, Nelson LM, Norris JM, et al. Epidemiology of environmental exposures and human autoimmune diseases: findings from a national institute of environmental health sciences expert panel workshop. *J Autoimmun* (2012) 39:259–71. doi: 10.1016/j.jaut.2012.05.002
- Selmi C, Leung PS, Sherr DH, Diaz M, Nyland JF, Monestier M, et al. Mechanisms of environmental influence on human autoimmunity: a national institute of environmental health sciences expert panel workshop. *J Autoimmun*. (2012) 39:272–84. doi: 10.1016/j.jaut.2012.05.007
- Parks CG, Miller FW, Pollard KM, Selmi C, Germolec D, Joyce K, et al. Expert panel workshop consensus statement on the role of the environment in the development of autoimmune disease. *Int J Mol Sci*. (2014) 15:14269–97. doi: 10.3390/ijms150814269
- Occupational Safety and Health Administration (OSHA), Department of Labor. Occupational exposure to respirable crystalline silica. Final rule. *Fed Regist*. (2016) 81:16285–890. <https://www.osha.gov/sites/default/files/laws-regis/federalregister/2016-09-01.pdf>

23. Zaghi G, Koga F, Nishihara RM, Skare TL, Handar A, Rosa Utiyama SR, et al. Autoantibodies in silicosis patients and in silica-exposed individuals. *Rheumatol Int.* (2010) 30:1071–5. doi: 10.1007/s00296-009-1116-z
24. Rocha-Parise M, Santos LM, Damoiseaux JG, Bagatin E, Lido AV, Torello CO, et al. Lymphocyte activation in silica-exposed workers. *Int J Hyg Environ Health* (2014) 217:586–91. doi: 10.1016/j.ijheh.2013.11.002
25. Parks CG, Cooper GS, Nylander-French LA, Sanderson WT, Dement JM, Cohen PL, et al. Occupational exposure to crystalline silica and risk of systemic lupus erythematosus: a population-based, case-control study in the Southeastern United States. *Arthritis Rheum.* (2002) 46:1840–50. doi: 10.1002/art.10368
26. Vupputuri S, Parks CG, Nylander-French LA, Owen-Smith A, Hogan SL, Sandler DP. Occupational silica exposure and chronic kidney disease. *Ren Fail.* (2012) 34:40–6. doi: 10.3109/0886022X.2011.623496
27. Cooper GS, Parks CG. Occupational and environmental exposures as risk factors for systemic lupus erythematosus. *Curr Rheumatol Rep.* (2004) 6:367–74. doi: 10.1007/s11926-004-0011-6
28. Schleiff PL. Surveillance for silicosis — Michigan and New Jersey, 2003–2011. *MMWR* (2016) 63:73–8. doi: 10.15585/mmwr.mm6355a7
29. Makol A, Reilly MJ, Rosenman KD. Prevalence of connective tissue disease in silicosis (1985–2006)-a report from the state of Michigan surveillance system for silicosis. *Am J Ind Med.* (2011) 54:255–62. doi: 10.1002/ajim.20917
30. Brown JM, Archer AJ, Pfau JC, Holian A. Silica accelerated systemic autoimmune disease in lupus-prone New Zealand mixed mice. *Clin Exp Immunol.* (2003) 131:415–21. doi: 10.1046/j.1365-2249.2003.02094.x
31. Brown JM, Pfau JC, Holian A. Immunoglobulin and lymphocyte responses following silica exposure in New Zealand mixed mice. *Inhal Toxicol.* (2004) 16:133–9. doi: 10.1080/08958370490270936
32. Brown JM, Schwanke CM, Pershouse MA, Pfau JC, Holian A. Effects of rotterlin on silica-exacerbated systemic autoimmune disease in New Zealand mixed mice. *Am J Physiol Lung Cell Mol Physiol.* (2005) 289:L990–8. doi: 10.1152/ajplung.00078.2005
33. Pfau JC, Brown JM, Holian A. Silica-exposed mice generate autoantibodies to apoptotic cells. *Toxicology* (2004) 195:167–76. doi: 10.1016/j.tox.2003.09.011
34. Sang A, Yin Y, Zheng YY, Morel L. Animal models of molecular pathology systemic lupus erythematosus. *Prog Mol Biol Transl Sci.* (2012) 105:321–70. doi: 10.1016/B978-0-12-394596-9.00010-X
35. Bates MA, Brandenberger C, Langohr I, Kumagai K, Harkema JR, Holian A, et al. Silica triggers inflammation and ectopic lymphoid neogenesis in the lungs in parallel with accelerated onset of systemic autoimmunity and glomerulonephritis in the lupus-prone NZBWF1 mouse. *PLoS ONE* (2015) 10:e0125481. doi: 10.1371/journal.pone.0125481
36. Calder PC. Functional roles of fatty acids and their effects on human health. *J Parent Ent Nutr.* (2015) 39:18S–32S. doi: 10.1177/0148607115595980
37. Calder PC. Very long-chain n-3 fatty acids and human health: fact, fiction and the future. *Proc Nutr Soc.* (2018) 77:52–72. doi: 10.1017/S0029665117003950
38. Winwood RJ. Recent developments in the commercial production of DHA and EPA rich oils from micro-algae. *OCL* (2013) 20:D604. doi: 10.1051/ocl/2013030
39. Adarme-Vega TC, Thomas-Hall SR, Schenk PM. Towards sustainable sources for omega-3 fatty acids production. *Curr Opin Biotechnol.* (2014) 26:14–8. doi: 10.1016/j.copbio.2013.08.003
40. Calder PC. Marine omega-3 fatty acids and inflammatory processes: effects, mechanisms and clinical relevance. *Biochim Biophys Acta* (2015) 1851:469–84. doi: 10.1016/j.bbali.2014.08.010
41. Pestka JJ. n-3 Polyunsaturated fatty acids and autoimmune-mediated glomerulonephritis. *PLEFA* (2010) 82:251–8. doi: 10.1016/j.plefa.2010.02.013
42. Lim BO, Jolly CA, Zaman K, Fernandes G. Dietary (n-6) and (n-3) fatty acids and energy restriction modulate mesenteric lymph node lymphocyte function in autoimmune-prone (NZB × NZW)F1 mice. *J Nutr.* (2000) 130:1657–64. doi: 10.1093/jn/130.7.1657
43. Jolly CA, Muthukumar A, Reddy Avula CP, Fernandes G. Maintenance of NF-κB activation in T-lymphocytes and a naive T-cell population in autoimmune-prone (NZB/NZW)F1 mice by feeding a food-restricted diet enriched with n-3 fatty acids. *Cell Immunol.* (2001) 213:122–33. doi: 10.1006/cimm.2001.1866
44. Bhattacharya A, Lawrence RA, Krishnan A, Zaman K, Sun D, Fernandes G. Effect of dietary n-3 and n-6 oils with and without food restriction on activity of antioxidant enzymes and lipid peroxidation in livers of cyclophosphamide treated autoimmune-prone NZB/W female mice. *J Am Coll Nutr.* (2003) 22:388–99. doi: 10.1080/07315724.2003.10719322
45. Kim YJ, Yokozawa T, Chung HY. Suppression of oxidative stress in aging NZB/NZW mice: effect of fish oil feeding on hepatic antioxidant status and guanidino compounds. *Free Rad Res.* (2005) 39:1101–10. doi: 10.1080/10715760500250083
46. Kim YJ, Yokozawa T, Chung HY. Effects of energy restriction and fish oil supplementation on renal guanidino levels and antioxidant defences in aged lupus-prone B/W mice. *Br J Nutr.* (2005) 93:835–44. doi: 10.1079/BJN20051440
47. Halade GV, Rahman MM, Bhattacharya A, Barnes J, Chandrasekar B, Fernandes G. Docosahexaenoic acid-enriched fish oil attenuates kidney disease and prolongs median and maximal life span of autoimmune lupus-prone mice. *J Immunol.* (2010) 184:5280–6. doi: 10.4049/jimmunol.0903282
48. Halade GV, Williams PJ, Veigas JM, Barnes JL, Fernandes G. Concentrated fish oil (Lovaza(R)) extends lifespan and attenuates kidney disease in lupus-prone short-lived (NZBxNZW)F1 mice. *Exp Biol Med.* (2013) 238:610–22. doi: 10.1177/1535370213489485
49. Robinson DR, Prickett JD, Makoul GT, Steinberg AD, Colvin RB. Dietary fish oil reduces progression of established renal disease in (NZB x NZW)F1 mice and delays renal disease in BXSb and MRL/1 strains. *Arth Rheum.* (1986) 29:539–46. doi: 10.1002/art.1780290412
50. Robinson DR, Xu LL, Tateno S, Guo M, Colvin RB. Suppression of autoimmune disease by dietary n-3 fatty acids. *J Lipid Res.* (1993) 34:1435–44.
51. Pestka JJ, Vines LL, Bates MA, He K, Langohr I. Comparative effects of n-3, n-6 and n-9 unsaturated fatty acid-rich diet consumption on lupus nephritis, autoantibody production and CD4+ T cell-related gene responses in the autoimmune NZBWF1 mouse. *PLoS ONE* (2014) 9:e100255. doi: 10.1371/journal.pone.0100255
52. Bates MA, Brandenberger C, Langohr II, Kumagai K, Lock AL, Harkema JR, et al. Silica-triggered autoimmunity in lupus-prone mice blocked by docosahexaenoic acid consumption. *PLoS ONE* (2016) 11:e0160622. doi: 10.1371/journal.pone.0160622
53. Reeves WH, Lee PY, Weinstein JS, Satoh M, Lu L. Induction of autoimmunity by pristane and other naturally-occurring hydrocarbons. *Trends Immunol.* (2009) 30:455–64. doi: 10.1016/j.it.2009.06.003
54. Brandenberger C, Rowley NL, Jackson-Humbles DN, Zhang Q, Bramble LA, Lewandowski RP, et al. Engineered silica nanoparticles act as adjuvants to enhance allergic airway disease in mice. *Part Fibre Toxicol.* (2013) 10:26. doi: 10.1186/1743-8977-10-26
55. Weening JJ, D'Agati VD, Schwartz MM, Seshan SV, Alpers CE, Appel GB, et al. The classification of glomerulonephritis in systemic lupus erythematosus revisited. *Kidney Int.* (2004) 65:521–30. doi: 10.1111/j.1523-1755.2004.00443.x
56. Tschanz SA, Burri PH, Weibel ER. A simple tool for stereological assessment of digital images: the STEPanizer. *J Microsc.* (2011) 243:47–59. doi: 10.1111/j.1365-2818.2010.03481.x
57. Fenton JI, Gurrzell EA, Davidson EA, Harris WS. Red blood cell PUFAs reflect the phospholipid PUFA composition of major organs. *Prostaglandins Leukot Essent Fatty Acids* (2016) 112:12–23. doi: 10.1016/j.plefa.2016.06.004
58. Bird AK, Meednu N, Anolik JH. New insights into B cell biology in systemic lupus erythematosus and Sjogren's syndrome. *Curr Opin Rheumatol.* (2015) 27:461–7. doi: 10.1097/BOR.0000000000000201
59. Espeli M, Bökers S, Giannico G, Dickinson HA, Bardsley V, Fogo AB, et al. Local renal autoantibody production in lupus nephritis. *J Am Soc Nephrol.* (2011) 22:296–305. doi: 10.1681/ASN.2010050515
60. Shen Y, Sun C-Y, Wu F-X, Chen Y, Dai M, Yan Y-C, et al. Association of intrarenal B-cell infiltrates with clinical outcome in lupus nephritis: a study of 192 cases. *Clin Dev Immunol.* (2012) 2012:967584. doi: 10.1155/2012/967584
61. Hamilton RF, de Villiers WJ, Holian A. Class A type II scavenger receptor mediates silica-induced apoptosis in Chinese hamster ovary cell line. *Toxicol Appl Pharmacol.* (2000) 162:100–6. doi: 10.1006/taap.1999.8799
62. Chao SK, Hamilton RF, Pfau JC, Holian A. Cell surface regulation of silica-induced apoptosis by the SR-A scavenger receptor in a murine lung macrophage cell line (MH-S). *Toxicol Appl Pharmacol.* (2001) 174:10–6. doi: 10.1006/taap.2001.9190
63. Hamilton RF, Thakur SA, Holian A. Silica binding and toxicity in alveolar macrophages. *Free Rad Biol Med.* (2008) 44:1246–58. doi: 10.1016/j.freeradbiomed.2007.12.027

64. Hamilton RF, Thakur SA, Mayfair JK, Holian A. MARCO mediates silica uptake and toxicity in alveolar macrophages from C57BL/6 mice. *J Biol Chem.* (2006) 281:34218–26. doi: 10.1074/jbc.M605229200
65. Holian A, Kelley K, Hamilton RF Jr. Mechanisms associated with human alveolar macrophage stimulation by particulates. *Environ Health Perspect* (1994) 102 (Suppl 10):69–74. doi: 10.1289/ehp.94102s1069
66. Iyer R, Hamilton RF, Li L, Holian A. Silica-induced apoptosis mediated via scavenger receptor in human alveolar macrophages. *Toxicol Appl Pharmacol.* (1996) 141:84–92. doi: 10.1016/S0041-008X(96)80012-3
67. Latch JN, Hamilton RF, Holian A, James JT, Lam C-W. Toxicity of lunar and martian dust simulants to alveolar macrophages isolated from human volunteers. *Inhal Toxicol.* (2008) 20:157–65. doi: 10.1080/08958370701821219
68. Migliaccio CT, Buford MC, Jessop F, Holian A. The IL-4R $\alpha$  pathway in macrophages and its potential role in silica-induced pulmonary fibrosis. *J Leukoc Biol.* (2008) 83:630–9. doi: 10.1189/jlb.0807533
69. Absher MP, Hemenway DR, Leslie KO, Trombley L, Vacek P. Intrathoracic distribution and transport of aerosolized silica in the rat. *Exp Lung Res.* (1992) 18:743–57. doi: 10.3109/01902149209031705
70. Yildirim-Toruner C, Diamond B. Current and novel therapeutics in the treatment of systemic lupus erythematosus. *J Allergy Clin Immunol.* (2011) 127:303–12. doi: 10.1016/j.jaci.2010.12.1087
71. Yap DY, Lai KN. The role of cytokines in the pathogenesis of systemic lupus erythematosus - from bench to bedside. *Nephrology* (2013) 18:243–55. doi: 10.1111/nep.12047
72. Manzi S, Sánchez-Guerrero J, Merrill JT, Furie R, Gladman D, Navarra SV, et al. Effects of belimumab, a B lymphocyte stimulator-specific inhibitor, on disease activity across multiple organ domains in patients with systemic lupus erythematosus: combined results from two phase III trials. *Ann Rheum Dis.* (2012) 71:1833–8. doi: 10.1136/annrheumdis-2011-200831
73. McMullen TPW, Lai R, Dabbagh L, Wallace TM, de Gara CJ. Survival in rectal cancer is predicted by T cell infiltration of tumour-associated lymphoid nodules. *Clin Exp Immunol.* (2010) 161:81–8. doi: 10.1111/j.1365-2249.2010.04147.x
74. Tucker LB, Uribe AG, Fenandez M, Vila LM, McGwin G, Apte M, et al. Adolescent onset of lupus results in more aggressive disease and worse outcomes: results of a nested matched case-control study within LUMINA, a multiethnic US cohort (LUMINA LVII). *Lupus* (2008) 17:314–22. doi: 10.1177/0961203307087875
75. Vos K, Thurlings RM, Wijbrandts CA, van Schaardenburg D, Gerlag DM, Tak PP. Early effects of rituximab on the synovial cell infiltrate in patients with rheumatoid arthritis. *Arthritis Rheum.* (2007) 56:772–8. doi: 10.1002/art.22400
76. Rosengren S, Wei N, Kalunian KC, Zvaifler NJ, Kavanaugh A, Boyle DL. Elevated autoantibody content in rheumatoid arthritis synovia with lymphoid aggregates and the effect of rituximab. *Arthritis Res Ther.* (2008) 10:R105. doi: 10.1186/ar2497
77. Koenig A, Thauinat O. Lymphoid neogenesis and tertiary lymphoid organs in transplanted organs. *Front Immunol.* (2016) 7:646. doi: 10.3389/fimmu.2016.00646
78. Clarke TC, Black LI, Stussman BJ, Barnes PM, Nahin RL. Trends in the use of complementary health approaches among adults: United States, 2002–2012. *Natl Health Stat Report* (2015) 79:1–16. <https://www.cdc.gov/nchs/data/nhsr/nhsr079.pdf>
79. Stussman BJ, Black LI, Barnes PM, Clarke TC, Nahin RL. Wellness-related use of common complementary health approaches among adults: United States, 2012. *Natl Health Stat Rep.* (2015) 79:1–12. <https://www.cdc.gov/nchs/data/nhsr/nhsr079.pdf>
80. Lokesh BR, Black JM, Kinsella JE. The suppression of eicosanoid synthesis by peritoneal macrophages is influenced by the ratio of dietary docosahexaenoic acid to linoleic acid. *Lipids* (1989) 24:589–93. doi: 10.1007/BF02535074
81. Calder PC. n-3 Fatty acids, inflammation and immunity: new mechanisms to explain old actions. *Proc Nutr Soc.* (2013) 72:326–36. doi: 10.1017/S0029665113001031
82. Saku N, Kobayashi J, Kitamura S. Eicosapentaenoic acid modulates arachidonic acid metabolism in rat alveolar macrophages activated by silica. *Prostaglandins Leukot Essent Fatty Acids* (1999) 61:51–4. doi: 10.1054/plef.1999.0073
83. Chen F, Sun SC, Kuh DC, Gaydos LJ, Demers LM. Essential role of NF- $\kappa$ B activation in silica-induced inflammatory mediator production in macrophages. *Biochem Biophys Res Commun.* (1995) 214:985–92. doi: 10.1006/bbrc.1995.2383
84. Koren HS, Joyce M, Devlin RB, Becker S, Driscoll K, Madden MC. Modulation of eicosanoid production by human alveolar macrophages exposed to silica *in vitro*. *Environ Health Perspect* (1992) 97:77–83. doi: 10.1289/ehp.929777
85. Kuroda E, Ishii KJ, Uematsu S, Ohata K, Coban C, Akira S, et al. Silica crystals and aluminum salts regulate the production of prostaglandin in macrophages via NALP3 inflammasome-independent mechanisms. *Immunity* (2011) 34:514–26. doi: 10.1016/j.immuni.2011.03.019
86. Panos RJ, Voelkel NF, Cott GR, Mason RJ, Westcott JY. Alterations in eicosanoid production by rat alveolar type II cells isolated after silica-induced lung injury. *Am J Respir Cell Mol Biol.* (1992) 6:430–8. doi: 10.1165/ajrcmb.6.4.430
87. Serhan CN. Pro-resolving lipid mediators are leads for resolution physiology. *Nature* (2014) 510:92–101. doi: 10.1038/nature13479
88. Yan Y, Jiang W, Spinetti T, Tardivel A, Castillo R, Bourquin C, et al. Omega-3 fatty acids prevent inflammation and metabolic disorder through inhibition of NLRP3 inflammasome activation. *Immunity* (2013) 38:1154–63. doi: 10.1016/j.immuni.2013.05.015
89. Schif-Zuck S, Gross N, Assi S, Rostoker R, Serhan CN, Ariel A. Saturated-efferocytosis generates pro-resolving CD11b low macrophages: modulation by resolvin and glucocorticoids. *Eur J Immunol.* (2011) 41:366–79. doi: 10.1002/eji.201040801
90. Lee HN, Kundu JK, Cha YN, Surh YJ. Resolvin D1 stimulates efferocytosis through p50/p50-mediated suppression of tumor necrosis factor- $\alpha$  expression. *J Cell Sci.* (2013) 126:4037–47. doi: 10.1242/jcs.131003
91. McCauley LK, Dalli J, Koh AJ, Chiang N, Serhan CN. Cutting edge: parathyroid hormone facilitates macrophage efferocytosis in bone marrow via proresolving mediators resolvin D1 and resolvin D2. *J Immunol.* (2014) 193:26–9. doi: 10.4049/jimmunol.1301945
92. EFSA. Scientific opinion on the extension of use for DHA and EPA-rich algal oil from *Schizochytrium* sp. as a novel food ingredient. *EFSA J.* (2014) 12:3843–60. doi: 10.2903/j.efsa.2014.3843

**Conflict of Interest Statement:** The authors declare that the research was conducted in the absence of any commercial or financial relationships that could be construed as a potential conflict of interest.

Copyright © 2018 Bates, Akbari, Gilley, Wagner, Li, Kopec, Wierenga, Jackson-Humbles, Brandenberger, Holian, Benninghoff, Harkema and Pestka. This is an open-access article distributed under the terms of the Creative Commons Attribution License (CC BY). The use, distribution or reproduction in other forums is permitted, provided the original author(s) and the copyright owner(s) are credited and that the original publication in this journal is cited, in accordance with accepted academic practice. No use, distribution or reproduction is permitted which does not comply with these terms.